Small-volume basaltic volcanoes: Eruptive products and processes, and posteruptive geomorphic evolution in Crater Flat (Pleistocene), southern Nevada

Greg A. Valentine[†]
Frank V. Perry
Don Krier
Gordon N. Keating
Richard E. Kelley
Allen H. Cogbill
Earth and Environmental Sciences Division, Los Alamos National Laboratory, Mail Stop D462, Los Alamos, New Mexico 87545, USA

ABSTRACT

Five Pleistocene basaltic volcanoes in Crater Flat (southern Nevada) demonstrate the complexity of eruption processes associated with small-volume basalts, and the effects of initial emplacement characteristics on posteruptive geomorphic evolution of the volcanic surfaces. The volcanoes record explosive processes ranging from "classical" Strombolian mechanisms to, potentially, violent Strombolian mechanisms. Cone growth was accompanied and sometimes disrupted by effusion of lavas from the bases of cones. Pyroclastic cones were built upon a gently southward-sloping surface and were prone to failure of their downslope (southern) flanks. Early lavas flowed primarily southward and, at Red and Black Cone volcanoes, carried abundant rafts of cone material on the tops of the flows. These resulting early lava fields eventually built platforms such that later flows erupted from the eastern (at Red Cone) and northern (at Black Cone) bases of the cones. Three major surface features—scoria cones, lava fields with abundant rafts of pyroclastic material, and lava fields with little or no pyroclastic material—experienced different posteruptive surficial processes. Failure to account for the different initial surface features can lead to erroneous conclusions about the relative ages of the surfaces based upon modern morphology. Conversely, the recognition of different volcanic surfaces provides the opportunity to study the effects of different initial properties upon posteruptive geomorphic processes. Contrary to previous interpretations that the individual volcanoes were emplaced by polycyclic eruptions (separated by thousands or tens of thousands of years), we argue that the Pleistocene Crater Flat volcanoes are monogenetic, each having formed in a single eruptive episode lasting up to a few years. We show that all eruptive products emanated from the areas of the volcanoes' main cones rather than from scattered vents, as inferred by previous workers. These conclusions provide insight into the processes associated with continental basaltic magmatism and information related to the geometry and timing of volcanic events, which is useful in risk assessments.

Keywords: scoria cone, basalt, lava flow, polycyclic, monogenetic, Strombolian, violent Strombolian.

INTRODUCTION

Despite being one of the most common types of continental volcanoes and presenting hazards to urbanized areas, such as Mexico City (Siebe et al., 2004), and to the proposed Yucca Mountain radioactive waste repository (e.g., Crowe, 1986; Dartevelle and Valentine, 2005), the eruptive processes of small-volume basaltic volcanoes (composed of cones, lava flows, and fallout deposits with total volumes of ~1 km^3 or less) have received relatively little attention in the volcanological literature. Much remains unknown about the ranges of explosive and effusive processes associated with their eruptions. The role of preexisting topography and the interaction between lava flows and cone building have not been explored in detail, nor has the influence of emplacement processes on posteruptive surficial processes. In this paper, we describe the physical volcanological and geomorphic aspects of five Pleistocene basaltic volcanoes in Crater Flat basin, southern Nevada. Although tephra fallout deposits that might have been associated with the volcanoes are largely obscured, many original volcanic features are preserved, and in some places, erosion has exposed important features in the interiors of the cones and lavas. We show that eruptions at each volcano formed a main cone, and lavas emanated from its base within a monogenetic framework that is consistent with historically observed scoria cone-forming events. This contrasts with previous interpretations that suggested that at least two of the volcanoes were polycyclic, with eruptions from multiple scattered vents (Vaniman and Crowe, 1981) and intravolcano temporal separations of ~10^3–10^4 yr (or greater) (Bradshaw and Smith, 1994). In addition, we discuss different modes of emplacement of the lavas, effects of lava flows on the structure of the main cones, and transitions in eruptive style. Finally, we show how the volcanic emplacement processes produced three types of volcanic surfaces that have subsequently experienced different geomorphic evolution; not accounting for these differences can lead to misinterpretation of relative ages of volcanic surfaces. Our work indicates that the three volcanic surfaces provide a test bed for quantifying the role of different initial conditions in determining the rates and types of geomorphic processes in a given climatic setting. In addition to providing basic information on the nature of continental basaltic volcanism, the

[†]E-mail: gav@lanl.gov.

GSA Bulletin; November/December 2006; v. 118; no. 11/12; p. 1313–1330; doi: 10.1130/B25956.1; 13 figures; 1 table; Data Repository item 2006173.

results of our study have important implications for the definition of potential future events in volcanic risk assessments at the proposed Yucca Mountain repository.

BACKGROUND

Crater Flat (Fig. 1) is an alluvial basin in the Basin-and-Range Province of the western United States. It is bounded to the east by ridges of tilted Miocene ignimbrite (Yucca Mountain) and to the west by uplifted Paleozoic sedimentary strata (Bare Mountain). Basaltic volcanism within the basin has occurred in three cycles. The first cycle, between 11.5 and 10 Ma, produced widespread basalt flows that are now mostly buried by alluvium (Stamatakos et al., 1997; Perry et al., 1998). The second cycle occurred in the southeastern quadrant of the basin ca. 3.7 Ma (Fleck et al., 1996; Perry et al., 1998). The third cycle produced a NE-trending arc of five volcanoes, which are the focus of this paper, SW and NE Little Cones, Red Cone, Black Cone, and Makani volcanoes (Fig. 1).

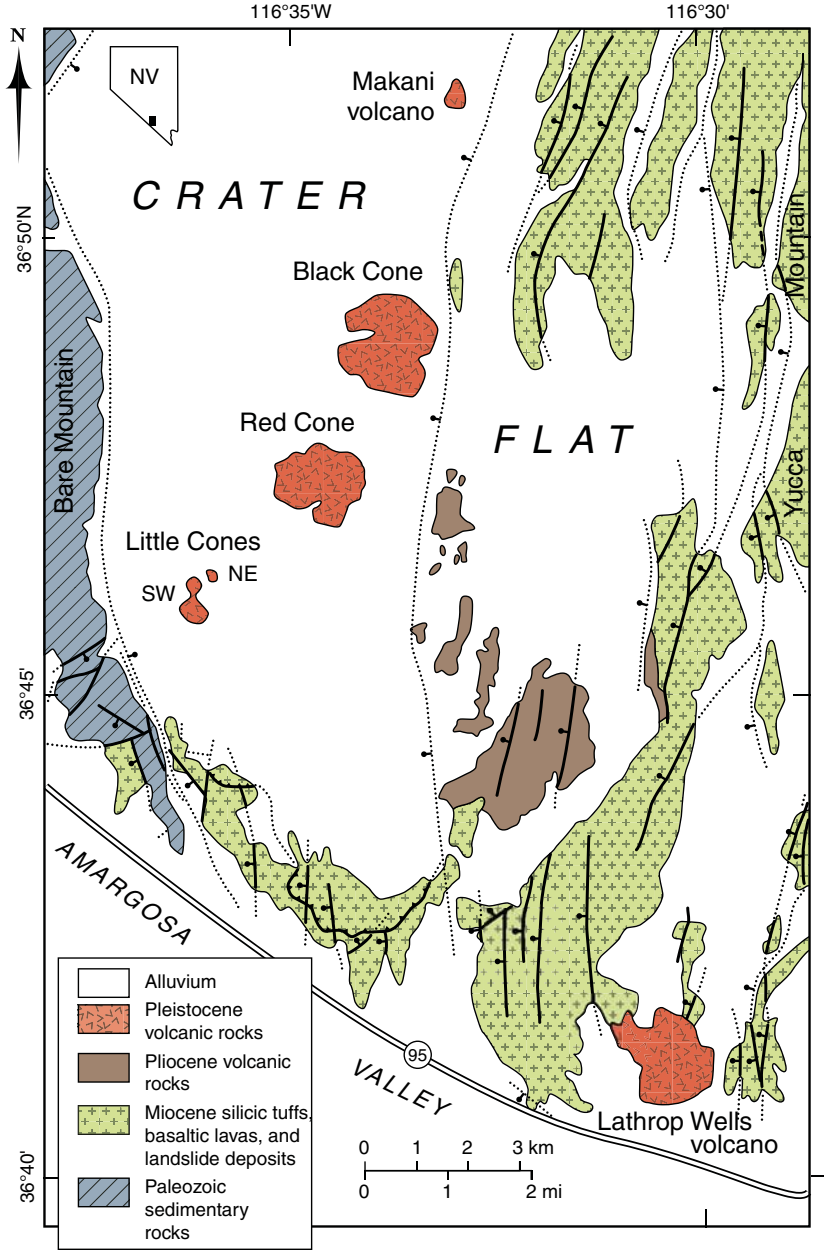

Figure 1. Simplified geologic map of Crater Flat and its immediate surroundings (modified from Vaniman and Crowe, 1981). Inset shows location of the study area within the state of Nevada.

(Note that Makani volcano is also referred to as "Makani Cone," "Northern Cone," and "Northernmost Cone" in the literature.) Six independent K-Ar and $^{40}Ar/^{39}Ar$ studies have been conducted since 1990 to determine the ages of these five volcanoes (Fig. 2), and the results are difficult to interpret. Age estimates for any one volcano typically have uncertainties of 100–200 k.y. and a large range of individual age determinations, leaving a detailed understanding of the age relationships between volcanoes uncertain, as well as the possibility of a span of ages at individual volcanoes. Flows of all of the volcanoes have reversed magnetic polarity, indicating that, if all the volcanoes are close to the same age, they are either older than 1.07 Ma or younger than 0.99 Ma (Fig. 2); for simplicity in this paper, we refer to the age of these volcanoes as ca. 1 Ma. The total volume of preserved eruptive products in the Pleistocene volcanic centers in Crater Flat is 0.15 km^3 (Table 1). Red Cone and Black Cone volcanoes account for ~75% of this volume and receive the most attention in this paper. The Lathrop Wells volcano, located ~5 km outside the southeast margin of Crater Flat, erupted ca. 80 ka (Heizler et al., 1999); its volcanological and geomorphic characteristics are reported elsewhere (e.g., Crowe et al., 1983; Wells et al., 1990; Valentine et al., 2005; Valentine and Harrington, 2006).

The eruptive products of the 1 Ma volcanic centers are sparsely porphyritic and are alkali basaltic to hawaiitic (trachybasaltic) in composition (Vaniman and Crowe, 1981; Vaniman et al., 1982; Bradshaw and Smith, 1994; Fleck et al., 1996; and Perry et al., 1998). Olivine is the principal phenocryst, with rare amphibole (mainly at Little Cones). Nicholis and Rutherford (2004) conducted experiments to determine phase equilibria and ascent rates for magma from SW Little Cone and Lathrop Wells volcanoes. They determined that SW Little Cone magma erupted at temperatures less than 975 °C with a source pressure of at least 175 MPa (depth greater than ~7 km). Dissolved-water content at depth must have been at least 3 wt% for amphibole to crystallize. Melt inclusions analyzed by Nicholis and Rutherford (2004) yielded H_2O contents mainly in the range of 1.2–1.7 wt% and as high as 3.5 wt% in one inclusion. Luhr and Housh (2002) reported values of 1.9–4.6 wt% H_2O and CO_2 contents up to 930 ppm from Red Cone and Lathrop Wells volcanoes.

Vaniman and Crowe (1981) and Bradshaw and Smith (1994) described the eruptive sequences of Red and Black Cone volcanoes. Both papers infer that mounds of pyroclasts scattered amongst the lava flows record the presence of multiple scattered vents, in addition to the main cone at each of the two volcanoes.

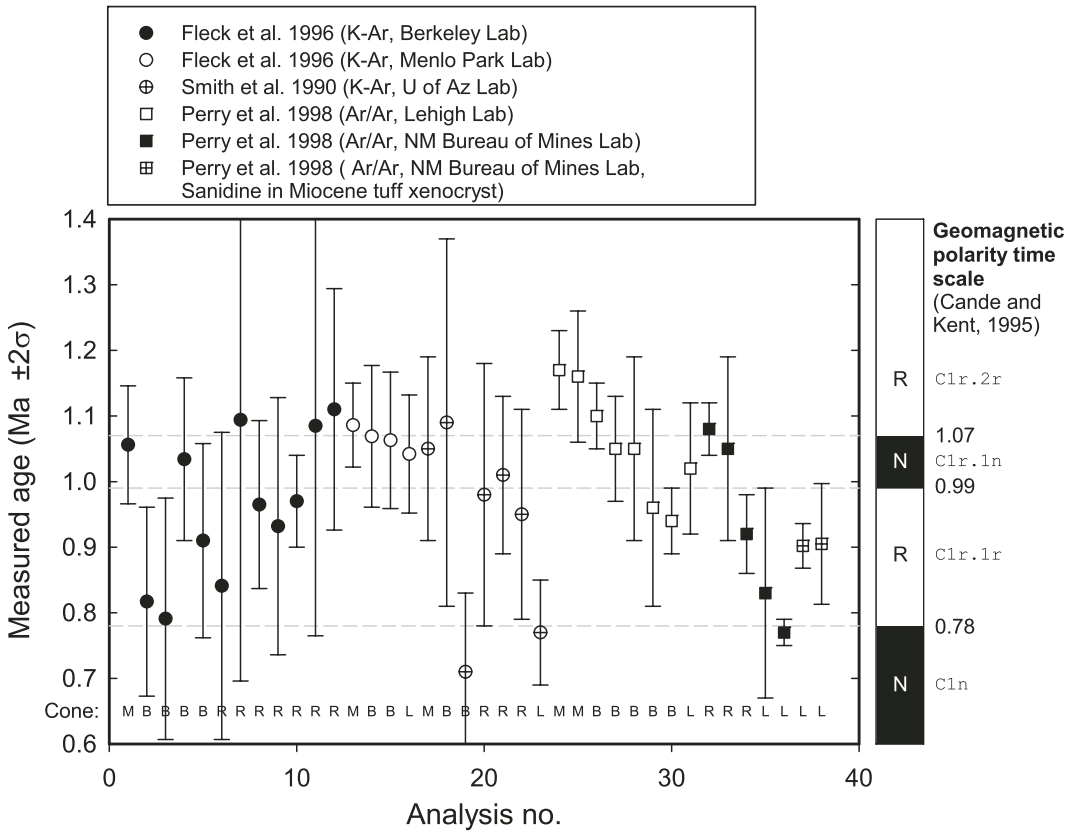

Figure 2. Summary of K-Ar and $^{40}Ar/^{39}Ar$ age determinations for the Quaternary basalts of Crater Flat. Errors bars are ±2σ. Age determinations are grouped by laboratory. M, B, R, and L labels for "Cone" near the bottom of the figure indicate that the corresponding age determination is for Makani volcano, Black Cone, Red Cone, or Little Cones, respectively.

However, the authors came to different conclusions with respect to timing of eruptive events. Vaniman and Crowe assumed a monogenetic history (i.e., a single eruptive episode of weeks to years in duration, during which all the features of a volcano are formed). Bradshaw and Smith promoted a polycyclic model with eruptive episodes separated by thousands or tens of thousands of years (or greater, but within the resolution of the age data shown in Fig. 2). Bradshaw and Smith (1994) argued that differences in morphology of lava flows, some having rather subdued margins and gullied surfaces compared to others, are the result of significant age differences between the flows. These arguments, along with arguments related to primary volcanic features that Bradshaw and Smith interpreted to represent polycyclic eruptive episodes, are addressed throughout this paper. Volcanological and geomorphic terminology used in the paper is defined in a supplement accessible online in the GSA Data Repository.[1]

[1]GSA Data Repository item 2006173, definition of volcanology and geomorphology terms used in this paper, is available on the Web at http://www.geosociety.org/pubs/ft2006.htm. Requests may also be sent to editing@geosociety.org.

RED CONE VOLCANO

Red Cone volcano (Fig. 3) consists of three major features: (1) a cone remnant that rises 87 m above the floor of Crater Flat (combined debris apron, lapilli-and-block, and spatter units in Fig. 3B), (2) a lava flow field that extends to the south and southwest of the cone remnant (the SW lava field), and (3) a lava flow field that extends to the south-southeast of the cone remnant (SE lava field).

Cone Remnant

The topographically highest part of Red Cone volcano is a roughly horseshoe-shaped remnant of in situ cone deposits (Fig. 4A) that exposes two main pyroclastic facies. Xenoliths

TABLE 1. ESTIMATED VOLUMES OF PLEISTOCENE VOLCANIC CENTERS IN CRATER FLAT

Volcano name	Volume (km^3)†	Brief description
Black Cone	0.061‡	Single cone with two lava flow fields
Red Cone	0.055	Single cone with two lava flow fields
Little Cones	0.03§	Two small cones, each with a lava flow field (mostly buried by alluvium) extending southward
Makani Cone	0.004#	Small lava field with minor pyroclastics

†Volumes were calculated by reconstructing a sloping planar paleosurface beneath each volcano (determined by elevation of points around the edge of each volcano, assuming that this is close to the contact between volcanic products and the paleosurface unless noted otherwise), and integrating the digital elevation data above that surface. The volume estimates do not account for distal fallout deposits that may have existed but are now obscured or missing due to posteruptive surficial processes.

‡Bradshaw and Smith (1994) estimated the volume of Black Cone volcano to be 0.067 ± 0.015 km^3.

§Combined volume of SW and NE Little Cone volcanoes and their lava flow fields. Value assumes that each of the two lava fields is 10 m thick and buried by an average of 10 m of alluvium.

#Assumes 5 m partial burial of volcanic products, in addition to those exposed on the surface.

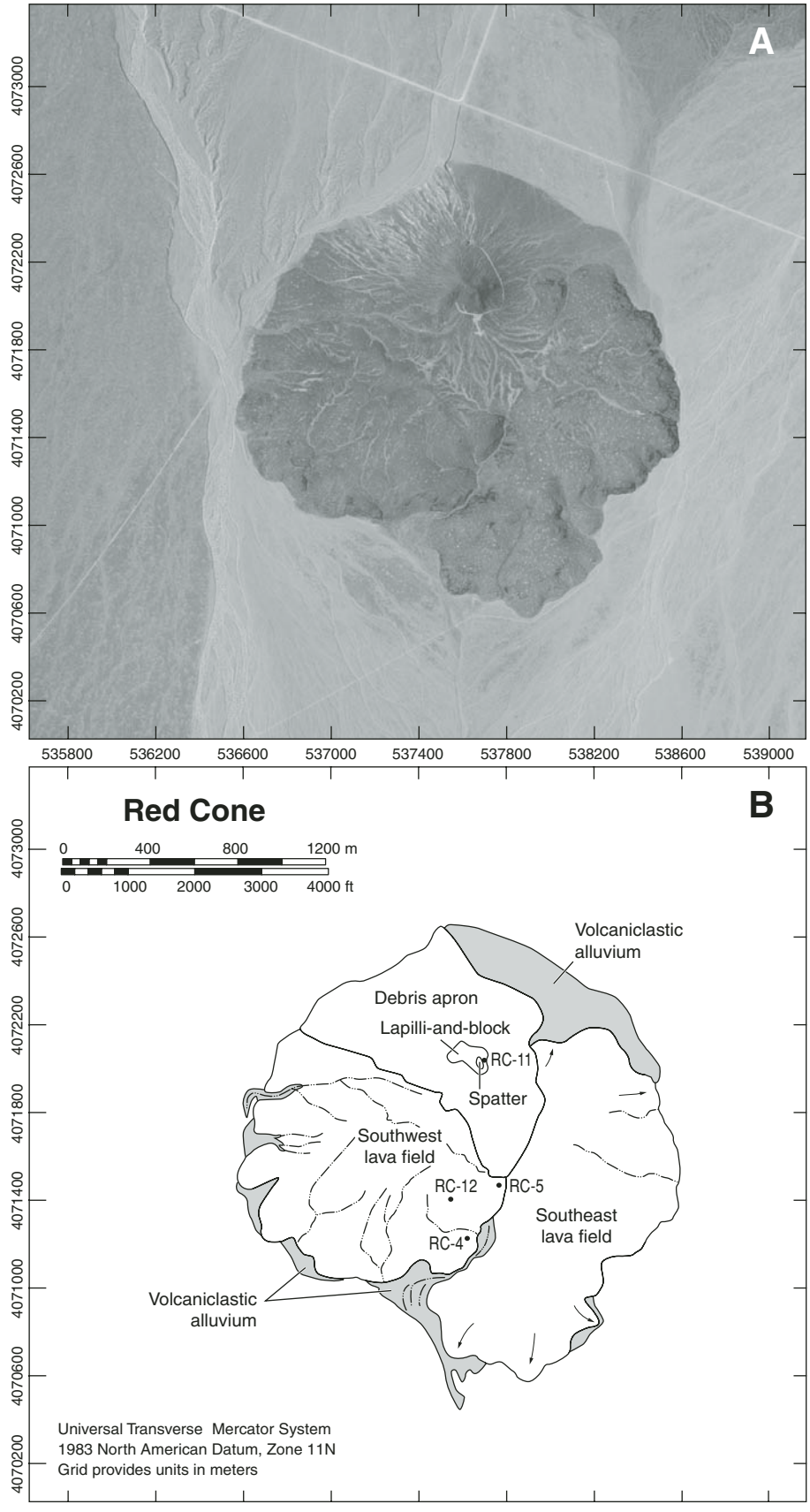

Figure 3. Air photo (A) and geologic map (B) of Red Cone volcano (arrows represent inferred flow directions of lavas).

are extremely rare in both of these facies—we observed only a few centimeter-sized xenoliths, probably derived from basin-fill sediments, in the entire cone remnant. Deposits on the west and northern parts of the cone remnant are mainly lapilli and small blocks, are clast supported, form crudely defined massive beds, and are partly welded—these deposits form the lapilli-and-block facies. Lapilli are poorly to moderately vesicular with mainly submillimeter vesicles and are blocky to subrounded in shape; many of these clasts likely are fragments of larger blocks or bombs that were recycled or churned due to avalanching of crater-wall material into the vent and subsequent re-ejection (McGetchin et al., 1974; Heiken, 1978). Blocks (and some bombs) are typically 20–30 cm in size and range from dense with blocky shapes to moderately vesicular clasts with fluidal shapes and cauliflower surface textures. Larger (up to ~50 cm) blocks and cauliflower bombs litter the surface where it is covered by colluvium but were not observed in place; these probably are a lag from eroded cone material.

Bed attitudes in the lapilli-and-block facies on the western part of the cone remnant are irregular but typically dip steeply (50–60°) toward the center of the apparent crater. The deposits are locally faulted into small blocks on the order of a few meters wide that retain the original bedding internally but that have undergone differing degrees of rotation. On the eastern side of the cone remnant, beds of this partly welded lapilli-and-block facies are nearly horizontal in attitude or dip shallowly back into the cone. These are broken into small fault or slump blocks. One small area on the east slope of the cone remnant (Station RC-11, Fig. 3B) exposes primary, nonindurated scoria lapilli with faint bedding that dips ~32° eastward (away from the center of the cone remnant). This represents primary, in situ material at the angle of repose that was deposited on the outer flanks of the cone during its growth.

A sequence of several meters of coarse lapilli, spatter, and fluidal bombs that forms individual beds ~1 m thick overlies the lapilli-and-block facies on the eastern summit. The beds alternate between partly welded to completely welded where clasts have coalesced to form massive, lava-like beds. These dip ~45° toward the north (strike varies around ~N75°W). We refer to these deposits as the spatter facies. The characteristics of this facies require a period of pulsing fountain eruptions where the relatively coarse clasts had a short flight time (minimum cooling) and a rapid accumulation rate (allowing for coalescence and welding of clasts). Deposition was likely very close, within some tens of meters, of a vent (see Head and Wilson, 1989; Sumner et al., 2005).

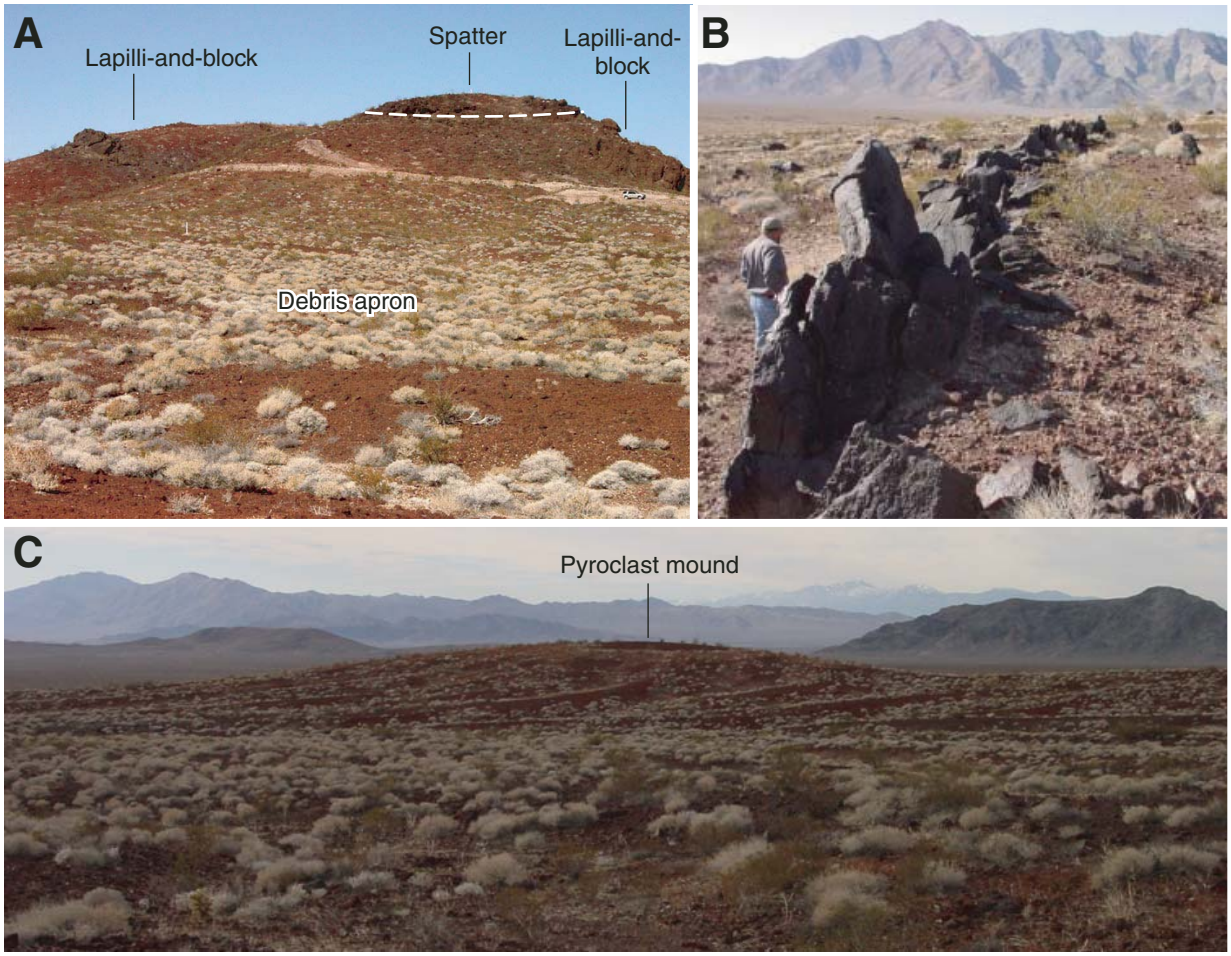

Figure 4. (A) Cone remnant at Red Cone volcano, viewed from surface of cone apron looking northward. Distance across photo is ~160 m. (B) Lava ridge on down-flow flank of a large pyroclast mound (Station RC-12). (C) Photograph taken from slopes of cone remnant looking to the south across the surface of the SW lava field, showing large pyroclast mound in the middle ground. Mound has a basal diameter of ~80 m.

An apron of material eroded from the cone surrounds the cone remnant, and the apron is in turn deeply rilled (Fig. 3A). The apron partly covers the two lava flow fields to the south and east and merges with the Crater Flat valley floor to the west and north.

Lava Flow Fields

Southwest Lava Flow Field

The SW lava flow field at Red Cone volcano fans out from the cone remnant to form a series of lava terraces that steps down toward the distal edge of the flows. The lavas flowed down the gentle (~20 m/km) south-southeast slope of the Crater Flat valley floor. The length:width ratio of the lava field is ~1:1 (length measured southward from the cone, width measured along the widest east-west dimension). The four main surface features on the lava field are: (1) relatively flat areas, (2) flow fronts or margins, (3) lava ridges, and (4) pyroclast mounds. Flat areas have a desert pavement of scoria lapilli (commonly ~1 cm in size, depending upon distance from the cone remnant) with variable quantities of block-size clasts (ranging from surface mosaic types DP-1 to BG-1 as described on a 560 ka lava flow at the Cima volcanic field by Wood et al., 2002, 2005). The blocks are typically angular in shape and are poorly to moderately vesicular. Beneath the pavement is a zone (depth unknown, but probably variable) of eolian sand and silt, which form a desert soil.

Flow fronts are partly obscured by alluvial deposits of reworked pyroclastic material that form relatively smoothly sloping surfaces to the surrounding valley floor, but where exposed, the fronts are steep, lobate, and composed largely of lava blocks on the order of decimeters in size. The terrace-like nature of the lava field is especially apparent along its margins, where each flow front forms a step (typically a few meters high) downward to the south and southwest.

Lava ridges are typically arcuate in shape (although some are roughly equant in map view, possibly representing tumuli), range from ~5–50 m in length, are a few decimeters to ~2 m wide, and rise up to 2 m above the surrounding surface. Internal textures in these ridges are dominantly nonvesicular to moderately vesicular, massive to platy-jointed lava. Although the ridges occur in a scattered fashion throughout the lava field, they are most abundant near flow margins, where they appear to be squeeze-up ridges, roughly parallel to the flow margin, caused by pulses of lava behind a slowing flow front. This interpretation is supported by observations where gullies have exposed flow interiors within ~200 m of the southern margin of the SW lava field. The flow interiors contain foliation patterns (due to vesicle concentrations or slide planes in the plastically flowing lavas)

that range from horizontal to upward-sweeping; these record ramping and squeezing up of lava near flow margins that is expressed on the surface by the lava ridges. Depending upon the degree of erosion, the lava ridges can be similar in appearance to exposed dikes—in a sense they are "rootless" dikes, since they are fed by the underlying lava flow rather than by a deeper magma reservoir. Two additional lava ridge features occur on the leading (southern) edges of pyroclast mounds (Fig. 4B). These are also arcuate and parallel the contours of their host mounds, and they resemble dikes.

Several mounds of pyroclastic debris, ranging from a few tens to ~200 m in basal diameter, rise 5–10 m above the SW lava field surface (e.g., Fig. 4C). The mounds have subdued, rounded surfaces and are littered to varying degrees with scoria lapilli, blocks, and bombs with eolian sand between the pyroclasts. In most cases, the tops of the mounds have the coarsest clasts, probably representing lag deposits, while smaller lapilli have been moved down the shallow slopes by surficial processes. Coarse clasts have a wide range of vesicularity and a range of surface textures, including ropy, fluidal textures (e.g., spindle bombs or bomb fragments) to blocky, although wind erosion has smoothed some features. Some large blocks are composed of agglutinate or basalt breccia. Bradshaw and Smith (1994, p. 168) stated that at Red Cone volcano "cinder mounds typically occur at the tail-end of individual flows, and thus represent actual vent sites." However, because posteruptive surficial processes have obscured many original lava features, we were not able to distinguish individual flows (in the sense of flow units) except perhaps as individual lobes at the distal margin of the lava field. Additionally, we observed pyroclast mounds out to the margin of the SW lava flow field, along its eastern side, and Bradshaw and Smith (1994) also mapped these. Bradshaw and Smith (1994, their Fig. 1) mapped several features in the mounds as "intrusives" into the pyroclast mounds of the SW lava field, supporting their hypothesis that the mounds were actual satellitic vents.

The abundance of large pyroclast mounds on the SW lava field promoted development of gullies in the topographic lows between mounds that now branch as rills onto the lower slopes of the mounds and have merged downstream with headward-eroding gullies that nucleated between marginal lava lobes. This drainage system supplies pyroclastic debris to the alluvial slopes that obscure some of the flow-margin features of the SW lava field, and it has locally incised the distal portions of the lava field to expose flow interiors, as mentioned already.

Southeast Lava Flow Field

The SE lava field spreads from the eastern base of the cone and extends southward (Fig. 3) with a length:width ratio of ~2:1 (flow length is measured north to south, in the dominant direction of flow). It appears to overlap the SW lava field where the two flows' margins come together at the apex of a small canyon that is the gap between the eastern and western margins of the two lava fields. The fact that the flows that fed the SE lava field first flowed eastward is also consistent with the SW lava field being emplaced first and forming a topographic high that diverted subsequent lavas. The top of the SE lava field is relatively flat compared to the SW lava field and locally is covered with a pavement dominated by lapilli-sized scoria with some small blocks (similar to surface mosaic type DP-1 of Wood et al., 2002, 2005), and eolian material beneath the pavement. The few pyroclast mounds that occur on the SE lava field rise only a few meters above the surroundings and tend to have flat tops that are armored with very mature desert pavements (Valentine and Harrington, 2006), although one or two small mounds, which are dominated by block-sized fragments of fluidal bombs, do have rounded tops.

The margins of the SE lava field are lobate in form and very steep, descending 25–30 m to the valley floor. Lobes have typical horizontal dimensions of ~40–100 m, and many have top surfaces that step down as terraces, each several meters high, toward their distal ends. We infer that the down-stepping terraces represent small lava breakouts from the toes of lobes (see also Pinkerton and Sparks, 1976), each reaching successively farther onto the desert floor. Similar to the lava lobes described for the SW lava field, the surfaces of those on the edge of the SE lava field are characterized by decimeter-sized lava blocks. A feature that is shared by all of the Pleistocene lava flow fields in Crater Flat is the common occurrence of arcuate lava ridges, parallel to and just inboard from the flow margins.

Drainage networks are less strongly developed on the SE compared to the SW lava field. This is likely due to the lesser initial topographic variation and less abundant pyroclastic debris on the SE lava field. Drainage development has been restricted to headward erosion of gullies that nucleated between lava lobes at the margin of the lava field.

Interpretation and Summary of Red Cone Volcano

The two pyroclastic facies in the cone record two principal cone-building eruptive mechanisms. The lapilli-and-block facies represents accumulation of primarily solidified and well-fragmented clasts even in very proximal locations. While the clasts were hot enough to sinter and form an indurated deposit in the crater, they were sufficiently cool to retain their blocky shapes. It is possible that this facies formed during periods of violent Strombolian eruption that alternated with steam explosions that ejected little juvenile material but that re-ejected previously erupted clasts (and block/bomb fragments) that had slumped into the vent. Some of the internal faulting and rotation within the lapilli-and-block facies may be due to slumping of deposits as cone material was rafted away on top of lava flows (discussed in the following paragraph) in addition to a potential component of slumping during posteruptive cone degradation. The spatter facies records more "classical" Strombolian eruptions (see, e.g., Valentine and Groves, 1996; Valentine et al., 2005). Each densely welded zone in this facies formed during a peak in the clast accumulation rate for a given Strombolian burst. Lack of exposure prevents direct observation of cone facies that may underlie the lapilli-and-block facies, and it is unclear whether erosion might have removed deposits above the spatter facies. It is likely that during much of the eruptive history of Red Cone volcano, the cone was horseshoe-shaped (open to the south) in map view.

Although both Vaniman and Crowe (1981) and Bradshaw and Smith (1994) inferred that pyroclast mounds scattered throughout the lava flow fields (particularly the SW lava field at Red Cone volcano) are remnants of vents, we favor an interpretation whereby these mounds are composed of proximal pyroclastic material rafted from the main cone (see also descriptions of rafted cone material at other small-volume basaltic volcanoes; Gutmann, 1979; Holm, 1987; Luhr and Simkin, 1993). Although interpretation of these features is complicated by the degree of posteruptive surface modification, we argue that this interpretation is consistent with several observations: (1) The tops of the coarse pyroclast mounds are rounded and preserve no evidence of an eruptive vent or crater. (2) The mounds cannot be linked to individual lava flow units and occur out to the distal margins of lavas. (3) Features in the main cone suggest that its crater opened to the south and that deposits in the cone may have experienced syneruptive slumping, as would happen if the cone was undermined as material rafted from its base. (4) Lava ridges or dike-like features on the inferred leading edge of some scoria mounds are very similar to lava squeeze-ups at the front of rafted "mesoblocks" on the 1986 lavas at Izu-Oshima volcano, Japan (Sumner, 1998). The squeeze-up features at Izu-Oshima resulted as lava from the fluid interior of the flow extruded through cracks in the chilled

lava surface because of the weight of the rafted material and deceleration of lava behind a slowing flow front. An additional piece of evidence that occurs at Black Cone volcano (discussed in the following section) is an exposure of the internal structure of a pyroclast mound showing that it consists of steeply tilted layers of scoria and spatter (similar to rafted cone material on lavas associated with the ca. 1 ka Sunset Crater volcano, Arizona; Holm, 1987).

Sumner's (1998) description of squeeze-ups at Izu-Oshima, which also occur near flow margins, detailed how the tops of the features in some cases have an outward-flaring structure caused by the plastic behavior of the rapidly cooling lava as it protruded above the flow surface. We have observed very similar squeeze-up features in lava lobes in the much younger, but compositionally similar, Lathrop Wells volcano, and Duncan et al. (2004) described the active development of such squeeze-ups at Mount Etna, Italy. Bradshaw and Smith (1994, p. 168) interpreted such a feature where it occurs along the eastern margin of the SW lava field as follows (at Station RC-5, see Fig. 2B): "Flow foliations and vesiculation in the top of one of the dike (*sic*) units suggests a mushroom-like shape that might be expected as a lava reaches the surface and initiates a new flow." (Note, there is no evidence for a presumed flow that was fed by the dike.) It seems likely that this feature is a lava squeeze-up (a rootless dike) from the core of the underlying flow, rather than a true dike related to a separate magmatic (polycyclic) event, as argued by Bradshaw and Smith (1994). Gutmann (1979) described similar features where lava squeeze-ups intruded overlying pyroclastic deposits produced later in the eruption sequence of the same vent in the Pinacate volcanic field.

As Red Cone grew, it was simultaneously cannibalized by lavas flowing from its southern perimeter that rafted away segments of cone material (similar to processes witnessed at Paricutín volcano, Mexico; see Luhr and Simkin, 1993). The rafted material was coarse-grained and rich in bombs and bomb fragments due to its origin close to the vent. Individual rafts may have retained their original bedding structures (Holm, 1987), particularly if there was any welding or agglutination, or in other cases, they may have been composed of piles of unstructured, loose debris; however, subsequent surficial processes have obscured differences between these features. Lava squeeze-ups formed on the leading edges of at least two rafts, as well as intruding the bottoms of rafts that were transported to the flow margins. This early phase of lava flows produced the SW lava field through a combination of stacking of flow units and inflation by successive injections of lava (as at Paricutín; Luhr and Simkin, 1993). Eventually the SW lava field became thick enough to divert subsequent lavas such that they initially flowed eastward until they cleared the SW lava platform, at which point they turned and flowed southward down the slope of the valley floor. These later flows accumulated to form the SE lava field. The SE lava field rafted much less material from the main cone, perhaps due to better stability or strength of the cone in the area of the SE flow vent (discussed in a later section), or because production of pyroclasts at the vent had waned or completely stopped during the SE flows.

After eruptions ceased, surficial processes gradually began to degrade the main cone. Rilling and downslope transport of cone deposits produced an apron of reworked scoria lapilli and blocks. The apron was in turn subject to rilling and a second generation of downslope transport that is in process today. The cone erosion processes were likely intimately tied to pedogenic processes, which introduced eolian sand and silt and eventually calcium carbonate zones in the upper tens of centimeters of the volcanic deposit in this arid to semiarid environment (Wells et al., 1985; McFadden et al., 1987; Valentine and Harrington, 2006). The erosional processes acted to give the cone a concave-upward profile, characteristic of highly degraded scoria cones (e.g., Wood, 1980b; Wells et al., 1990; Hooper and Sheridan, 1998), although we note that at least on its southern side, the cone may have had an initially concave profile due to the large quantity of material rafted away on the SW lava field.

The surfaces of the two lava fields evolved in somewhat different manners. The SW lava field, with its abundance of pyroclast mounds, had a combination of relief and loose debris that promoted relatively faster and more extensive development of drainage networks and alluvial aprons or "fans" at the mouths of gullies. Where the SW lava field did not have pyroclast mounds on its top, its surface evolution involved the gradual smoothing of the rough lava surface by eolian deposition in low spots and by weathering of high features (see Wells et al., 1985). The SE lava field, on the other hand, had much less initial topographic variation and less loose debris on its surface, and simply has undergone gradual smoothing with associated soil and desert pavement development, such that it now forms a relatively flat-topped platform. Both the SE lava field and the flat parts of the SW lava field are currently at Stage B in the surface modification scheme of Wells et al. (1985). Some drainage network development has occurred on the surface of the SE lava field where there are three subdued mounds, but for the most part, its erosion is dominated by very slow headward erosion of gullies between marginal lava lobes. Relatively little transport of loose debris from the central parts of the SE lava field has resulted in substantially less accumulation of alluvial fans or aprons that would obscure or smooth the edge of the lava field.

BLACK CONE VOLCANO

Black Cone volcano (Fig. 5) shares many of the characteristics of Red Cone, including the presence of a single main cone, rising 118 m above the surrounding desert floor, and two (possibly three) lava flow fields (see also Bradshaw and Smith, 1994), the first of which flowed south from the cone and has many pyroclast mounds, and the second of which spread around the northern base of the cone.

Cone Remnant

Although Black Cone proper at first glance appears to be a relatively complete cone, nearly all the in situ primary pyroclastic deposits that crop out on the cone are inward-dipping. This implies that a large volume of cone material that formed outward-dipping deposits has been removed by erosion. Most of the surface of the cone is covered with colluvium that has been indurated by pedogenic carbonate buildup, but exposures of primary volcanic deposits indicate that there are two main pyroclastic facies (Fig. 6). The predominant one, which occupies the lower ~80% of the cone, forms the lapilli-and-bomb facies (e.g., Station BC-1, Fig. 5B). Bedding in this facies ranges from massive to crudely defined by bomb horizons to lenticular and inversely graded grain avalanche beds; dips are typically 25–30° into the cone. Scoria lapilli are moderately vesicular and are predominantly blocky and angular in shape. The clast-supported framework of lapilli, which is nonwelded to slightly sintered, contains variable portions of larger bombs. The bombs are most commonly a few decimeters in length (parallel to crude bedding) and around one decimeter thick, although some ribbon bombs are as long as 1.4 m and rare ovoid bombs are over 2 m in diameter. Many bombs enclose blocky scoria lapilli (accretionary bombs; Heiken, 1978), likely caused as fluid bombs landed on the scoriaceous slopes and enfolded scoria as they rolled or slumped back into the vent to be re-ejected or simply as they rolled or slid into their final resting places. Dense blocks several decimeters in diameter also occur in this facies but are less common than bombs.

The upper ~20% of Black Cone is dominated by alternating zones of partly to densely welded spatter (e.g., Station BC-2, Fig. 5B), forming a spatter facies that is similar to that at the top

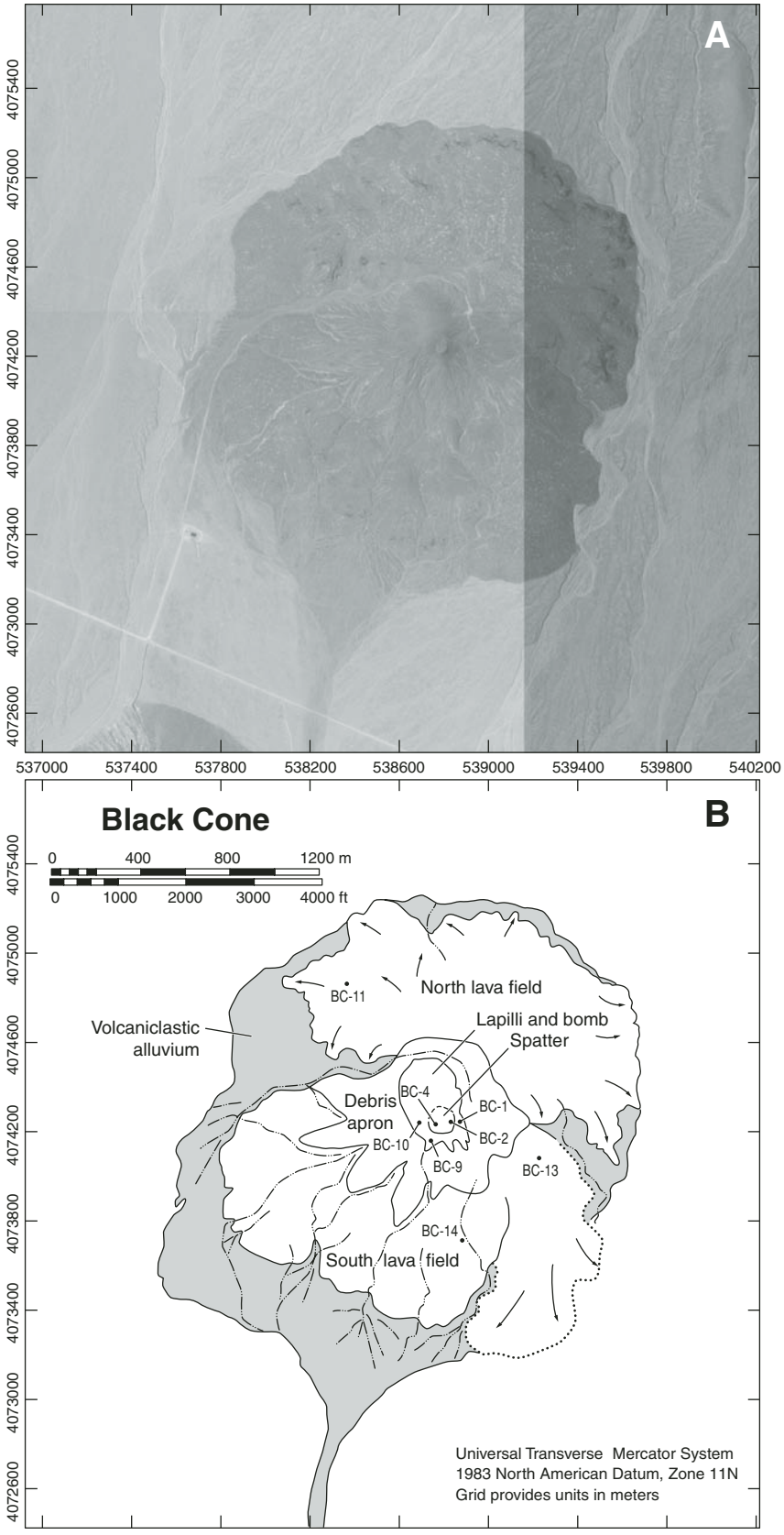

Figure 5. Air photo (A) and geologic map (B) of Black Cone volcano. Dotted line shows a lava field that is somewhat distinct because of its low profile, but we have lumped it with the south lava flow field in the text.

of Red Cone. The transition from lapilli-and-bomb to spatter facies may be a lateral transition instead of, or in addition to, a vertical transition; stratigraphically lower deposits are also farther away from the central vent area due to the slopes of the cone remnant. Thicknesses of ledge-forming welded horizons range from one spatter clast thickness (~10 cm) to ~2 m. Thicker beds, which also have the densest welding, tend to grade laterally over distances of 20–30 m to less welded zones with poorly defined bedding. The gradation typically occurs as a gradual thinning of the densely welded middle zone of a layer, increasing distinctness of clast outlines, and increasing abundance of lapilli relative to spatter and bombs. These features record deposition from asymmetric, short-lived spatter fountains. Locally, the thicker, densely welded zones have swirling textures indicative of some rheomorphic flow (i.e., rootless or clastogenic lavas). The spatter facies bedding dips concentrically inward toward the center of an ~75-m-diameter, bowl-shaped crater at the summit of Black Cone. Gullying on the southwest side of the crater has exposed deposits relatively close to its low point, and these are dominated by a 4-m-thick bed of densely welded spatter (Station BC-4, Fig. 5B) that grades laterally over 10–20 m into a less-welded zone. Previous authors (Vaniman and Crowe, 1981; Bradshaw and Smith, 1994) have referred to this as a lava lake. However, a lava lake would normally be expected to have a bottom contact that conforms to the crater walls and floor, a flat top, and a relatively massive interior throughout its extent. This feature near the summit of Black Cone is simply another local, densely welded spatter zone rather than a true lava lake.

Crustal xenoliths are rare at Black Cone, but there is a horizon in the spatter facies that contains relatively abundant (estimated at a few percent by volume), white, vesiculated xenoliths with margins that indicate potential melting into the basalt host. These xenoliths are probably derived from the alluvial sediments that fill Crater Flat basin. Their presence in deposits that were produced by dominantly magmatic (Strombolian) eruptions (see following discussion) underscores the observation that shallow crustal xenoliths do not necessarily record a locus of hydrovolcanic explosions in the volcanic feeder system (Valentine and Groves, 1996).

The angular unconformity that forms the contact between crater-filling (inward-dipping) and cone-slope-forming (outward-dipping) deposits is exposed in two places (Stations BC-9, 10; Fig. 5B). These limited exposures and the patterns of bed orientations suggest that the cone may have had a crater that was open to the south-southwest during early phases, which

subsequently healed, so that its final phases formed the relatively simple, circular crater that is indicated by the inward-dipping beds of the spatter facies at the summit of the cone remnant. Bradshaw and Smith (1994, p. 168) argued that the presence of a purported caliche layer along one of the angular unconformities supported their polycyclic interpretation, but did not provide a location. The only feature that we were able to find that resembles such a caliche layer is a layer of coarse ash along an unconformity that appears to have high calcium carbonate content (Station BC-9, Figs. 5B and 6). However, this is due to pedogenic processes on the modern surface, where carbonate accumulation can vary as a function of the host material grain size. Larger scoria lapilli in the surrounding exposures are commonly coated with white carbonate, especially on their undersides, that is left after the evaporation of infiltrated rain water, while ash layers tend to hold water in the pores between clasts until the water evaporates, leaving carbonate material that is evenly distributed throughout the deposit. Thus, the "caliche layer" does not record a significant (polycyclic) time break. The angular unconformity is simply one that is so commonly associated with scoria cone construction, with inner and outer slopes, periods of slumping and healing, and changes in geometry (e.g., McGetchin et al., 1974).

The cone remnant has a concave-upward profile in most quadrants, is deeply rilled on its flanks, and is surrounded by an apron of reworked pyroclastic debris that is also rilled. A gully system that cuts into the southwest flanks of the cone remnant exposes some scoria and bomb deposits near the base of the cone that have poorly defined bedding that appears to dip shallowly (10–20°) away (southward) from the cone. These likely are exposed deposits of the debris apron rather than primary deposits.

Lava Flow Fields

South Lava Flow Field

The south lava field consists of a relatively low-lying, flat-topped area on its eastern part (possibly a separate lava field, but not further distinguished here; Fig. 5B) and a larger area that has several large pyroclast mounds. The length:width ratio is ~1:2. In general, the pyroclast mounds are similar to the mounds on the SW lava field at Red Cone volcano. Most have shallow slopes and gently rounded tops that are littered with coarse (in some cases meter-sized) fluidal bomb fragments, scoria lapilli, and blocks. One mound has a beveled top that is littered with relatively dense lava blocks scattered among a "matrix" of large scoria lapilli; this mound may have originated as a high lava surface (e.g., a tumulus) that was covered with fallout scoria, rather than being a more easily modified mound of pyroclastic debris. A mound near the eastern part of the south lava flow field (Station BC-13, Fig. 5B) is littered with blocks and boulders of moderately welded agglutinate. Some of the larger blocks retain crude internal bedding, but there is no systematic orientation from one block to another. This is consistent with an origin by rafting of proximal pyroclastic facies from the main cone and disintegration of the material as it was carried atop a lava flow, rather than the mound being a vent in which bedding orientations should vary systematically around the mound. In common with the SW lava field at Red Cone, the south lava field at Black Cone volcano flowed from the base of the cone southward along the gentle slope of Crater Flat.

Posteruptive surface features on the south lava field are also similar to the SW lava field at Red Cone. Gullies formed in topographic lows between pyroclast mounds on the interior parts, and between flow lobes at the margin, of the lava field. In some places, the gullies have exposed interior features of pyroclast mounds. One excellent example (Station BC-14, Figs. 5B and 7A) exposes steeply tilted (~80° northward toward the main cone) beds similar to those found in the main cone remnant; they are consistent with an origin of the mound by rafting of cone material where original bedding was preserved but rotated and tilted as it traveled atop a lava flow (e.g., Holm, 1987; Sumner, 1998). Rills branch from the main gullies up onto the flanks of scoria mounds, and this drainage network in turn delivers pyroclastic debris from the interior of the lava field to its margins where it is actively accumulating as small alluvial fans or aprons that obscure the marginal features of the lava field.

North Lava Flow Field

The north lava field's length:width ratio is ~1:2, similar to that of the south lava field. A range of flow structures can be distinguished, even though the surface of the lavas has been modified. These include both arcuate lava ridges and circular or equant blisters or tumuli (e.g., Station BC-11 and vicinity, Fig. 5B) that appear to be due to squeeze-up processes in the active flows.

The north lava field forms a thicker platform than the south lava field, and several features provide clues to its complex emplacement processes. Broad terraces—each a few meters high and with steep, arcuate margins covered with basalt blocks (flow edges)—on the top of the lava field may record stacking of lava flows along channel areas. Stacking can result if a time interval between lava pulses is sufficient to solidify channel-filling lava so that later pulses flow on top of it (e.g., Kilburn and Lopes, 1991), and by channel overflows (perhaps as described by Rossi, 1997), as may occur if lava flux exceeds the local carrying capacity of a channel. In one location (~700–800 m directly north of the summit of Black Cone), a patch of coarse pyroclastic debris inferred to have rafted from the cone is partly overridden by a lava flow unit, also recording stacking as an important mechanism for building of the lava platform.

Lava lobes along the outer margin are commonly 40–100 m long and 20–40 m wide. Top surfaces of most of these lobes step down as terraces to the valley floor (e.g., Fig. 7B), representing, as with the lavas at Red Cone volcano, successive breakouts from the toes of the lobes. The fact that these lobes protrude from the main, thick lava platform suggests that a significant portion of lava transport was through a tube network beneath the surface, and breakout along the margins was an important mechanism by which the lava field widened and extended away from its vent area. This in turn implies that some of the thickness of the north lava field may be the result of inflation, as well as stacking of flows, as at Paricutín (Luhr and Simkin, 1993) and Etna (Duncan et al., 2004). In one case, a narrow (~10–15-m-wide) tongue of lava, with preserved levees on either side of a narrow central channel, appears to extend ~60 m from a terrace on the top of the lava platform toward the marginal lobes, partly overlapping and draping them. This also suggests a complex combination of subsurface transport within the lava field, breakout, and overlapping of lava flow units. We infer that these mechanisms worked in varying proportions in all the Pleistocene lava fields in Crater Flat, but the north lava field at Black Cone volcano better exhibits emplacement features because it is thicker and higher-standing as a result of its lavas having advanced up slope on the valley floor.

Posteruptive geomorphic features at the north lava field are similar to those of the SE lava field at Red Cone. Much of the top of the lava field is relatively flat as a result of original low spots having been filled with eolian sediment, and high spots having been broken down by mechanical weathering (Stage B of Wells et al., 1985). Desert pavements of lapilli-size clasts are locally developed, but in many areas the surface is dominated by angular (often somewhat smoothed by wind erosion) blocks of lava with eolian sediment and smaller lava clasts between. It is likely that these surfaces never had pyroclastic deposits on them, and the surface clasts are derived directly from lava surface rubble and weathered fragments of lava crags (similar to surface mosaic type BG-1 of Wood et al., 2002, 2005). Surfaces between

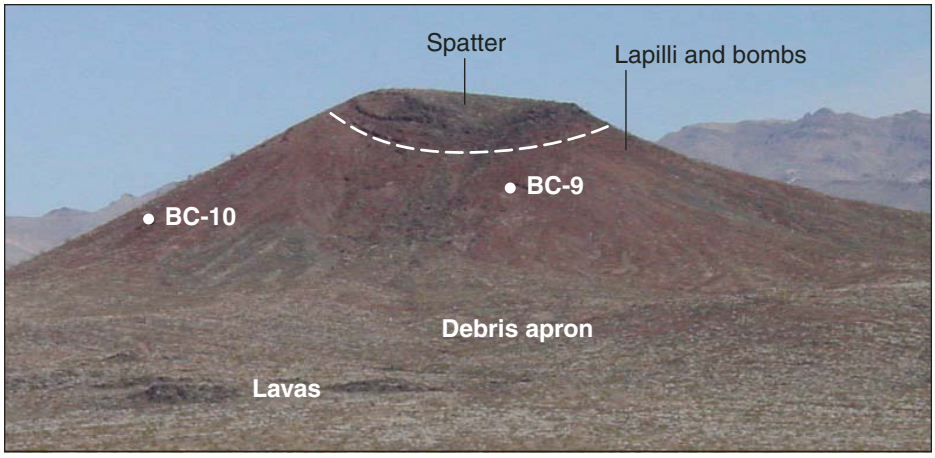

Figure 6. Photograph of Black Cone (viewed from the south) showing location of lapilli, block, and bomb facies (lower cone), spatter facies (upper cone), upper reaches of debris apron, and location (BC-9, -10) of unconformities between outward- and inward-dipping beds (most exposures are of inward-dipping beds).

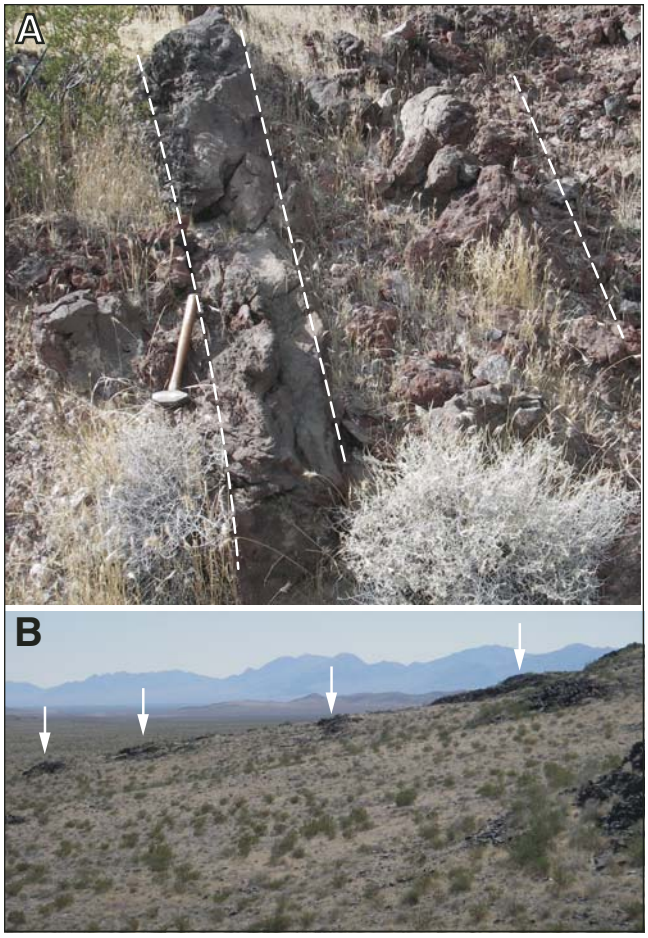

Figure 7. Features of Black Cone lavas. (A) Interior of pyroclast mound exposed by deep gully along its eastern margin (Station BC-14), showing steeply tilted beds of densely welded spatter (next to hammer) and less-welded agglutinate beds. (B) Terrace-like down-stepping of a lava lobe toward the valley floor due to successive breakouts (arrows) along eastern edge of north lava field. Lateral distance from left-most arrow to right-most arrow is ~100 m.

lava terraces are smooth and variably paved, sloping gently downward toward the next lowest terrace. Although there is some drainage development between marginal lava lobes, most of the interior of the lava field is free of gullies or rills.

Interpretation and Summary of Black Cone Volcano

The overall eruptive sequence of Black Cone volcano is similar to that of Red Cone volcano. Pyroclastic facies in the cone remnant preserve an evolution from eruption of relatively well-fragmented material that was cool and brittle (except for large bombs) upon deposition even very near to the vent, forming the lapilli-and-bomb facies, to eruption of coarse spatter. The lapilli-and-bomb facies may have resulted from eruptions with sustained, high-standing columns approaching a violent Strombolian mechanism, although recycling and breaking-up of large clasts by avalanching in the vent area probably had an important role in producing this facies as well. The spatter facies represents a later phase of weak, asymmetric bursts or short-lived fountains of lava. The cone may have had an open horseshoe shape during part of its eruptive history that was filled in or healed by later pyroclastic activity that terminated with a bowl-shaped crater where the cone remnant's summit is now.

Early lavas emanated from the southern base of the cone. The lavas spread southward following the gentle slope of the valley floor and rafted significant quantities of cone material with them, probably simultaneous with explosive activity, such that the lava field's surface was partly covered with fallout lapilli. As the south lava field thickened and spread laterally (eastward and westward), it reversed the slope at the base of the cone such that the later north lava field flowed northward. The north lava field spread and thickened by a combination of stacking and overlapping of flow units and tongues, and inflation with marginal breakouts. This lava field rafted very little cone material and may have occurred after the most dispersive explosive activity (corresponding to the lapilli-and-block facies of the cone remnant) had ceased, as reflected in the lesser abundance of fallout lapilli on its surface. The spatter facies in the cone may have been contemporaneous with the north lava field.

The three main features of Black Cone volcano (cone remnant, south lava field, north lava field) each had different characteristics due to different eruption and emplacement processes, and have each undergone somewhat different posteruptive geomorphic evolution. The

outward-dipping slopes of the cone have been removed, primarily through development of rills and runoff, to form a reworked apron around the cone remnant. This apron is in turn deeply rilled, and its deposits are being gradually remobilized to lower elevations. The south lava flow, with its abundance of rafted cone fragments, had an initially hilly surface covered with loose pyroclastic debris. A combination of gully development in low spots between mounds, rilling of the sides of the mounds, and headward erosion of gullies that nucleated between marginal lava lobes, produced an extensive drainage network and transported much pyroclastic debris to the margins of the lava field. This reworked debris is now accumulating as small alluvial fans and aprons that obscure the original lava margins. The north lava field was relatively flat to begin with. Combined accumulation of eolian sediment and mechanical weathering of crags and small highs have smoothed original lava surface roughness. Fluvial erosion and reworking is mainly limited to gullies that nucleated between marginal flow lobes, and the paucity of easily remobilized pyroclastic debris has left the steep flow margins relatively clearly defined.

LITTLE CONES

Description

Little Cones consists of two cone remnants, the SW and NE cones, the summits of which are separated by ~380 m (Fig. 8). Because of their location at the southern end of Crater Flat, alluvial sediments have buried most of the two lava flow fields associated with these cones, but the extent of the lava fields is known from ground magnetic and aeromagnetic data (Fig. 9; Stamatakos et al., 1997; Connor et al., 1997; Perry et al., 2005).

The SW cone remnant rises 24 m above the surrounding desert floor. A small quarry pit at the northwest base of the cone exposes clast-supported beds of highly vesicular, coarse, blocky scoria lapilli. The beds dip outward, away from the center of the cone remnant, at ~30°. Many of these beds are lenticular and inversely graded, and they show no evidence of welding. The most likely emplacement mechanism is a combination of fallout from sustained eruption columns with avalanching down the cone flanks. The higher flanks of the cone remnant are littered with scoria lapilli and bombs. Bombs are decimeters to ~1 m in size and commonly preserve some fluidal textures, although some have cauliflower surface textures. The abundance of bombs on the surface could be due to a lag effect as smaller lapilli have been removed by runoff. The cone remnant is deeply rilled and

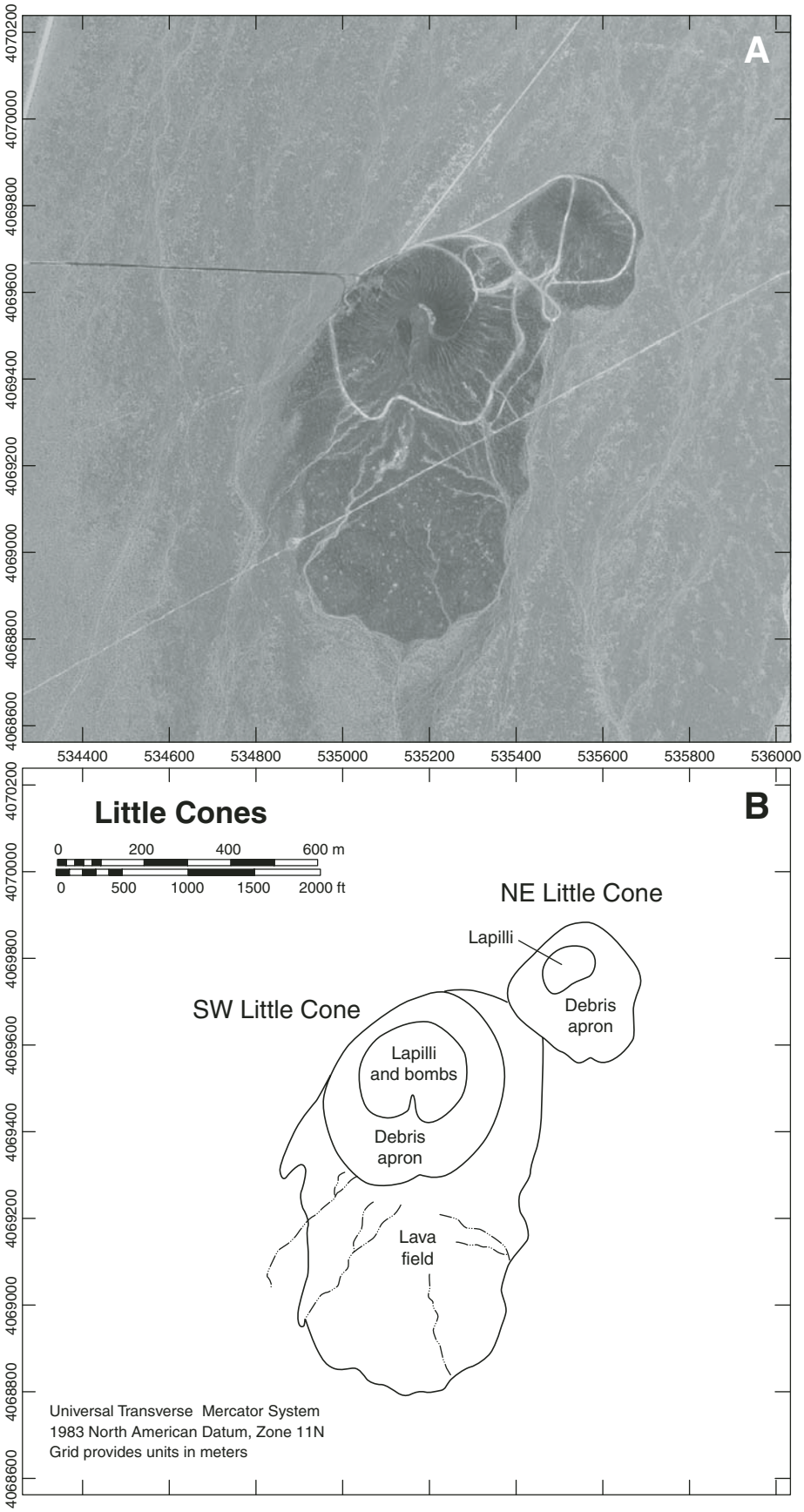

Figure 8. Air photo (A) and geologic map (B) of Little Cone volcanoes.

surrounded at its base by an apron of reworked pyroclastic material that is also rilled.

The SW cone's crater is open to the south, and its lava field extends primarily in that direction; it is likely that the crater was open to the south during eruption and lavas erupted from the south and southwest base of the cone as indicated by aeromagnetic data (Fig. 9). Most of the lava flow field exposure is actually a surface with varying amounts of scoria lapilli and lava blocks, with eolian sand between the clasts. However, near its east edge, small lava ridges, probably representing squeeze-up structures as described in the previous sections, do protrude above the surface, indicating that the top of the lavas is near the surface (Fig. 9). The length: width ratio of this lava field is ~1:1.

The NE cone remnant is a 15-m-high hill with no crater. It is littered with scoria lapilli and is rilled. The buried lava flow field from NE Little Cone extends 2 km to the south (length:width ratio of ~2:1). It is possible that the lack of a crater remnant at NE Little Cone reflects advanced degradation of the cone by rafting of material on top of the lava flows, or simply by posteruptive erosion. However, since the surrounding alluvial surface is aggrading, and therefore the base level for cone degradation is rising, it seems unlikely that posteruptive erosion at NE Little Cone would have been more rapid than at other Pleistocene volcanoes in the basin.

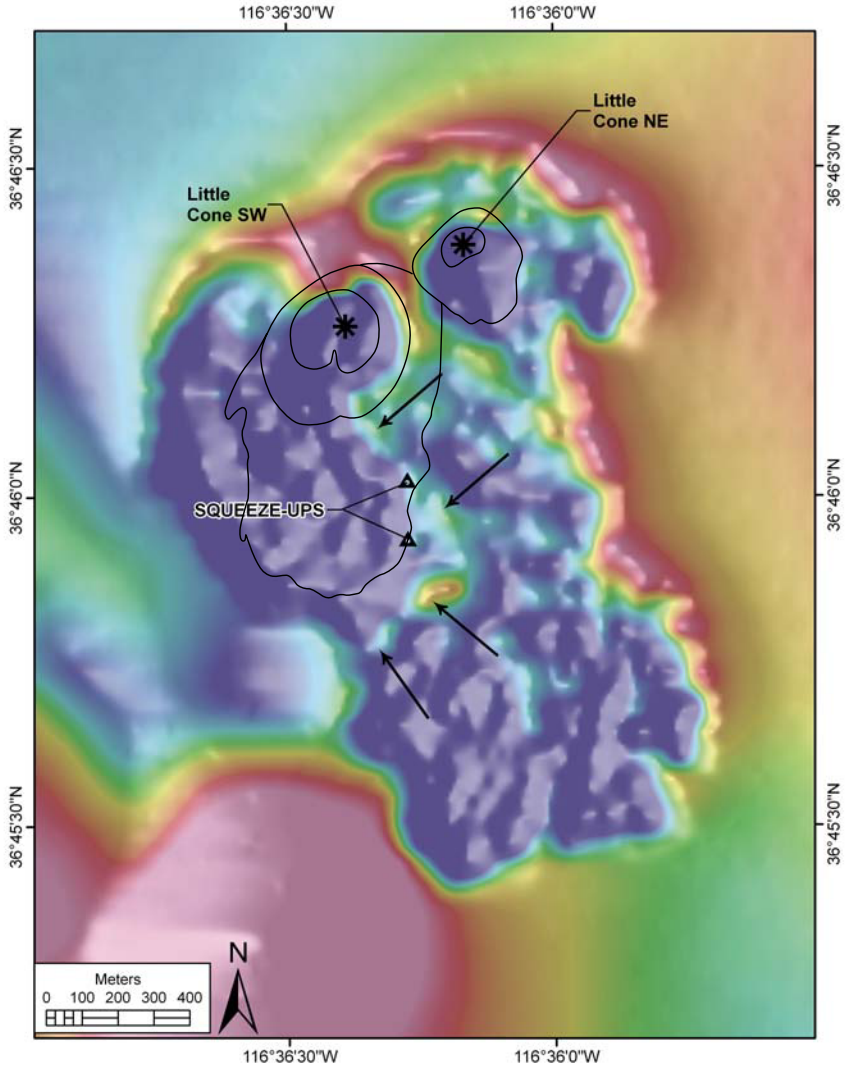

Figure 9. Aeromagnetic anomaly map of Little Cone volcanoes (colors range from blue, representing strong reversed polarity magnetization, to red, which represents strong normal magnetization). Areas characterized by high-amplitude, small-wavelength variations in magnetization are buried lava fields. One lava field spreads south to southwest of SW Little Cone, while another extends ~2 km directly south from NE Little Cone. Asterisks represent centers of cone remnants, and triangles are locations of lava squeeze-ups. Contacts from geologic map (Fig. 8B) are shown for comparison. Arrows point to eastern margin of the lava field associated with SW Little Cone.

Interpretation and Summary of Little Cones

Little Cones appear to be similar to Red and Black Cone volcanoes in that they each have a cone that was likely built by a combination of Strombolian and violent Strombolian mechanisms, and lavas that extend southward down the valley slope. However, the Little Cones volcanoes appear to have one lava flow field each, rather than later ones that were diverted around early lavas. Incompatible trace-element compositions of bombs from the two cones differ significantly, which is consistent with an interpretation that each cone represents a separate eruptive episode. Sr, Th, and La, for example, have concentrations that are 45%–70% higher at SW Little Cone than at NE Little Cone (Perry et al., 1998).

Aeromagnetic data combined with the surface exposures south of SW Little Cones allow a reasonable interpretation of the eruptive sequence of these two cones. We interpret the eastern lava flow field, from NE Little Cone, to represent the younger eruption, because it appears to have flowed around and past the western lava flow field from SW Little Cones (Fig. 9). The SW Little Cones lava flow field appears to have a top that is near the present surface, as suggested by the surface features described herein. This implies that the western flow is thicker than the more completely buried eastern flow. Stamatakos et al. (1997) used ground magnetic data to model the eastern flow as a 10-m-thick flow buried by 15 m of alluvium. If this is correct, and if the base of both lava fields is at the same elevation, the thickness of the western flow (which nearly reaches the surface) is ~25 m.

MAKANI VOLCANO

Description

Makani volcano is a very small eruptive center that forms a subdued mesa with no cone structure. Its top is ~5 m above the surrounding terrain, and the map-view diameter is ~500 m (Fig. 10). The eastern half is littered with scoria lapilli and fluidal bomb fragments and eolian sand and silt between clasts, has a slightly rounded top, and has some radiating rills in its surface that supply sediment to a narrow debris apron around the eastern part of the volcano.

The western half has a relatively flat surface with lava blocks and eolian sediment between clasts, and a steep western margin of lava lobes.

Interpretation

We interpret Makani volcano to have formed by eruption along a short (200–300 m), roughly N-S–trending fissure located within the lapilli-and-bomb extent in Figure 10B. Weak fountaining produced the bombs and scoria and possibly a low-profile pyroclastic construct in the eastern part of the volcano, while lavas effused and flowed a short distance westward. Posteruptive surface processes have been dominated by rilling and reworking of loose pyroclastic material on the eastern part of the volcano. The western part is a small lava platform in Stage B of Wells' et al. (1985) surface evolution scheme, and, like the SE lava field at Red Cone and the north lava field at Black Cone volcanoes, it has experienced little erosion except for gullies between marginal flow lobes.

DISCUSSION

Eruptive and Emplacement Processes

Our work shows that the lower exposures at Red and Black Cone volcanoes may record violent Strombolian mechanisms, while the upper deposits record later phases of explosive activity that were dominated by weak Strombolian bursts. Gutmann (1979) described cones in the Pinacate volcanic field that exhibit upward increases in abundance of coarse blocks and bombs and capping sequences of welded agglutinate that appear to be very similar to the sequences we describe. He attributed the variation to the interplay between magma flux and bubble nucleation and growth processes. Previous authors have referred to the upper spatter facies at Red and Black Cone volcanoes as deposits of Hawaiian eruptions (e.g., Vaniman and Crowe, 1981; Crowe et al., 1983; Crowe, 1986; Bradshaw and Smith, 1994; Perry et al., 1998). However, the alternating degree of welding between beds and the limited lateral extent of densely welded deposits in very proximal locations indicate asymmetric, low, temporally discrete fountains more akin to Strombolian eruptions than to Hawaiian eruptions, which produce sustained lava fountains (e.g., Parfitt, 2004) and more extensive welded facies. The presence of cauliflower surface textures on bombs in the lapilli-and-block facies at Red Cone, along with a relatively higher abundance of rounded (recycled) clasts, may reflect a component of magma-water interaction and steam explosions in the vent. Other than this, and a

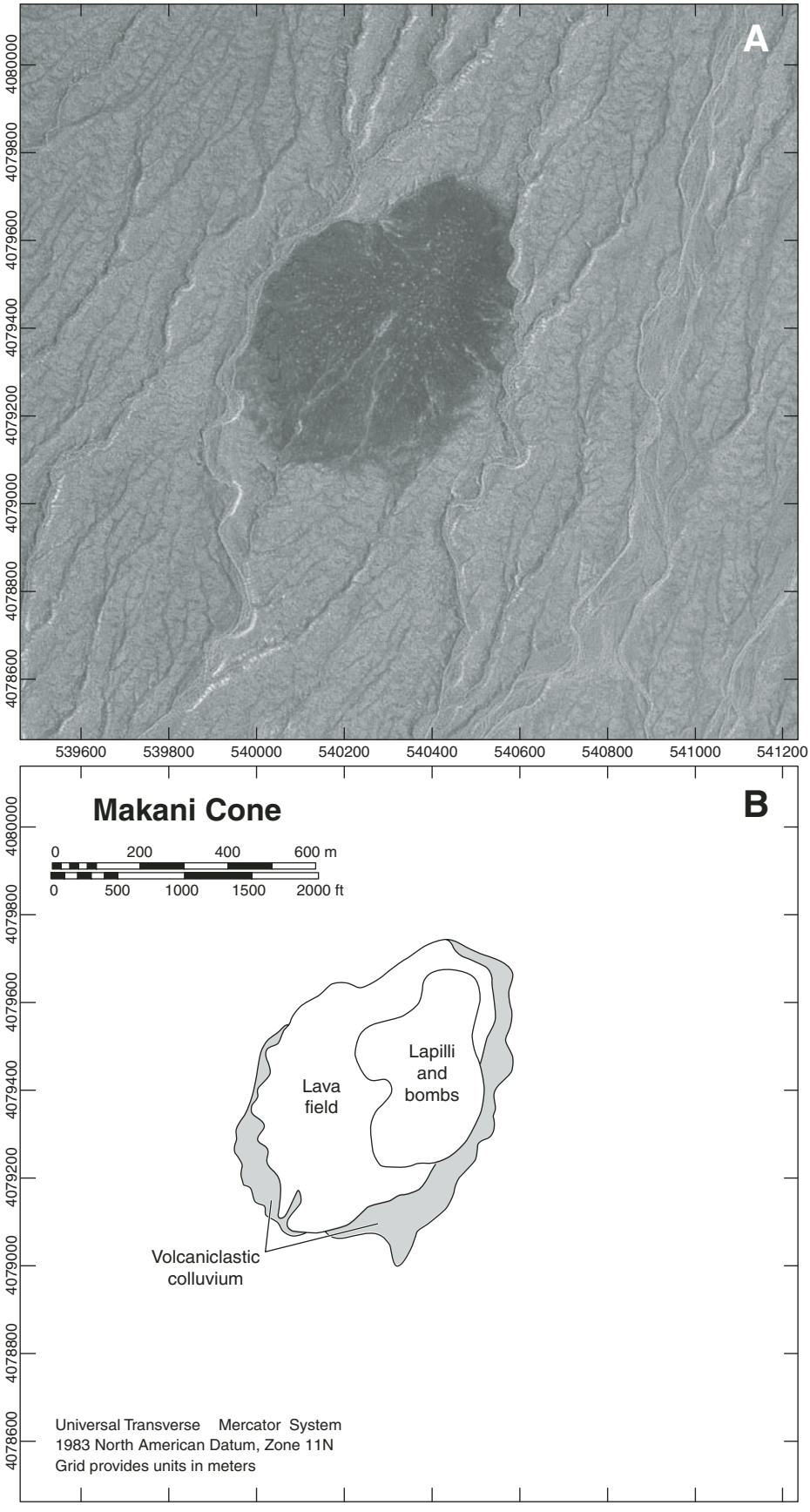

Figure 10. Air photo (A) and geologic map (B) of Makani volcano.

few cauliflower bombs at SW Little Cone, there is no evidence of any substantial hydrovolcanic activity in the 1 Ma Crater Flat centers.

All of the volcanoes discussed here, except for Makani volcano, produced lava flows that first erupted from the southern bases of the main cones, and spread south-southwestward down the shallow slope of the Crater Flat valley floor (the estimated southward topographic gradient varies from 25 m/km beneath Black Cone to 20 m/km beneath Red Cone to and 16 m/km beneath the two Little Cone volcanoes). The resulting lava fields at Red Cone, Black Cone, and SW Little Cone volcanoes extend 600–800 m away from their vents, while the lava field at NE Little Cone extends ~2 km. The length of NE Little Cone's lava field must reflect a relatively higher effusion rate (~1–3 m^3/s) compared to the other volcanoes (<1 m^3/s; cf. Walker, 1973). With these rates, the SW and south lava fields at Red and Black Cone volcanoes, respectively, would have been emplaced over periods of 9–12 mo.

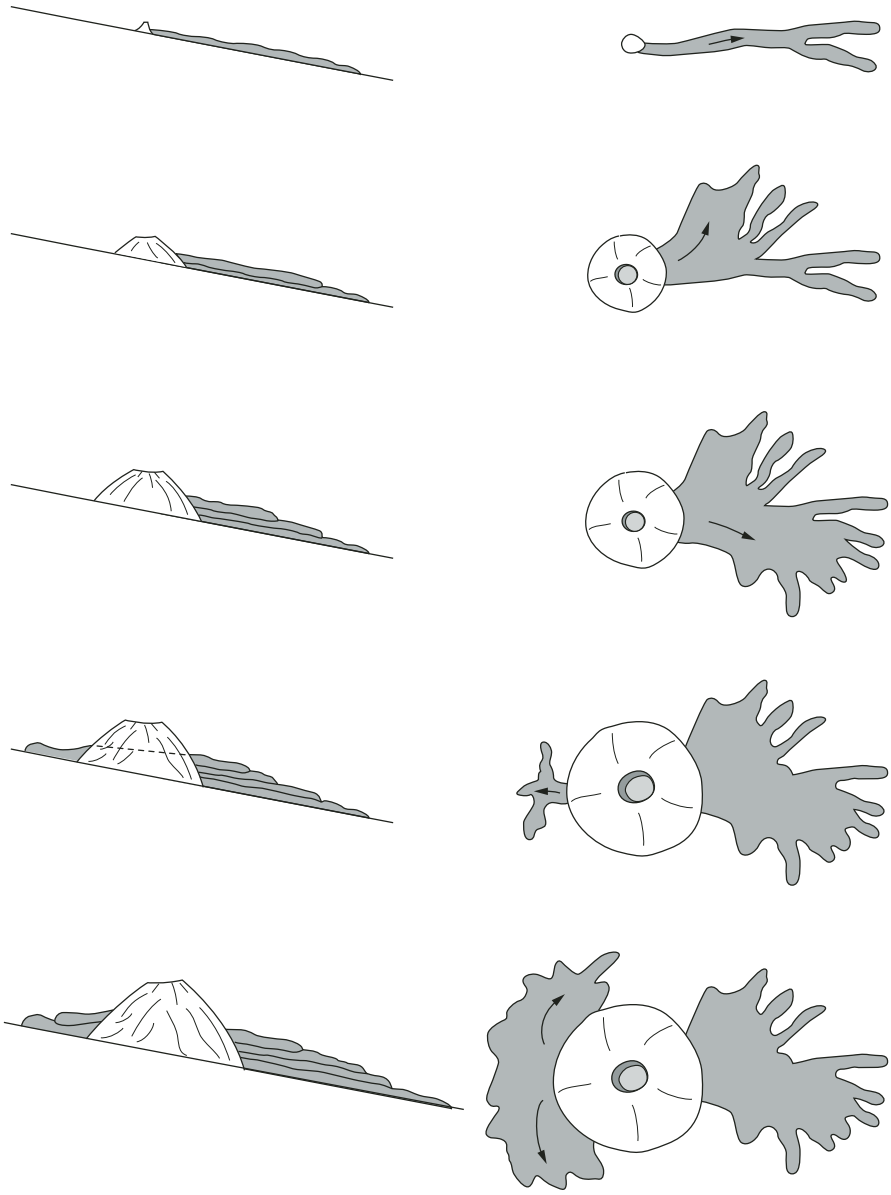

Figure 11. Sequence of events for developing fan-shaped lava flow fields simultaneously with cone growth on a gently sloping surface. Left column shows cross-section view, and right column shows map view at corresponding stages. The beginning of the sequence is shown at the top with initial lava flow from a small cone. Subsequent pulses of lava build a fan-shaped lava field. When the thickness of the lava field is sufficient, subsequent lava effusion is diverted to a different location along the cone base (bottom figures).

In detail, the flux may have been variable; it may be that for these small lava fields, the effusion occurred as discrete pulses that achieved higher effusion rates but only for short periods of time. The small length:width ratios for the early lava fields at Red and Black Cones could be explained by the following model (Fig. 11). Discrete pulses of lava first flowed directly downhill. These flows solidified during a non-effusive or weakly effusive period, forming a small platform (perhaps a few meters high) that was sufficient, given the gentle paleoslope, to divert the subsequent batch of flows to the side, so that, over time, the field spread laterally as a fan around the south side of a given cone. Lava pulses that were separated by insufficient time for the previous flows to solidify might have inflated those flows, or pushed new extrusions of lava from the toes of marginal lobes. Pulses that were separated by enough time for previous flows to solidify, but that had low effusion rates, may have traveled across the top of the previously built flows for short distances after which they solidified to form a terrace on the top of the growing platform. Thus, a lava field was built in a fan-like manner, where the radial distance from the vent to the margin was determined by peak effusion rates and durations of lava pulses, while the circumferential spread was determined by some minimum period between pulses (sufficient to allow solidification of the just-previous pulse) and the thickness of flow units relative to the slope of the depositional surface. Once the footprint of such a lava fan was covered with flows, stacking and inflation might have continued to thicken the lava field until its top was sufficiently high to essentially reverse the slope around the base of the cone (which was likely to have been growing as all the above was taking place). At this stage, if effusive activity continued, lava broke out from some new location around the base of the cone to form a new lava field (the SE and north lava fields at Red and Black Cone volcanoes, respectively). If effusive activity ceased before this stage, the volcano had only one lava field that extended from its downhill side.

The later lava fields at Red and Black Cones grew in different manners. At Red Cone volcano, the SE lava field appears to have welled out of the southeastern base of the cone. After growing a short distance (~400 m) eastward across the valley floor, it was able to catch the southward paleoslope and grow mainly in that direction for a distance of 1.6 km, with a lesser degree of lateral spreading compared to the earlier SW lava field, such that its length:width ratio is ~2:1. In contrast, the north lava field at Black Cone

appears to have vented from the northern base of the cone. Because its lavas were flowing northward against the paleoslope, individual pulses or flow units were easily diverted laterally, and the resulting length:width ratio is ~1:2. We also infer that a significant component of the north lava field's thickness is due to inflation as lavas were intruded into the interior of the platform as it thickened due to the limited uphill flow capability of the lavas.

We have argued that pyroclastic mounds observed in association with lavas are not separate vents but are masses of material rafted from the main cones, and a final point with respect to emplacement processes focuses on the fact that these mounds are most abundant on the early lava fields at Red and Black Cone volcanoes, compared to the later lava fields. In our discussion of Red Cone, we speculated that the later (SE) lava field vented from a stronger part of the cone, or that production of pyroclasts at the vent had waned or completely stopped during emplacement of the SE lava field. The first possibility is related to the observation that the cones were built upon a sloping surface (see schematic cross-section views in Fig. 11). The downhill (south-southwest) flanks of the cones would be weaker (perhaps in a state of relative tension) than the uphill sides, which would be in effect buttressed by the paleosurface. Although the elevation difference between the base of the cones on their uphill and downhill sides would have only been on the order of 10–20 m, this may have been sufficient to promote cone failure and rafting on lavas emanating from the downhill cone bases. Lava flow speeds might have been faster when emanating from the downhill side, which would also promote rafting. The Lathrop Wells volcano was also formed on a southward-sloping surface, and it exhibits the same relationships of preferential rafting with its early, southward-emplaced, lava field (Valentine et al., 2005). Gutmann (2002) pointed out that a large number of scoria cones in the Pinacate volcanic field that were built upon a sloping paleosurface are breached on their downhill sides by lavas that carried away significant quantities of cone material as rafts. This suggests that the process of cone deconstruction by rafting is an important, general process in the development of small basaltic volcanoes that are emplaced upon sloping surfaces.

An issue that cannot be definitively resolved about the Pleistocene Crater Flat volcanoes is whether significant fallout tephra deposits extended beyond the immediate vicinities of the pyroclastic cones. The volumes of lava and cone material at Red Cone and Black Cone volcanoes are very similar to the lava and cone volume at the ca. 80 ka Lathrop Wells volcano (0.05 km^3; Valentine et al., 2005). Red and Black Cones expose pyroclastic sequences that potentially evolved from early violent Strombolian to late-stage, weak Strombolian eruptions; this is typical of many scoria cones around the world (Wood, 1980a; Gutmann, 1979) but is an opposite trend to that at Lathrop Wells volcano (Valentine et al., 2005). However, because other features of the three volcanoes are very similar, it seems reasonable to postulate that Red and Black Cone volcanoes may originally have had laterally extensive fallout deposits similar to that associated with Lathrop Wells (~0.04 km^3; Valentine et al., 2005). Similarly, the two Little Cones volcanoes may have had laterally extensive fallout deposits, though probably not as large as Red and Black Cone volcanoes, assuming that the fallout volume was proportional to cone and lava volumes.

Posteruptive Surficial Processes

Different eruptive and emplacement processes at the Pleistocene centers in Crater Flat produced three major surface types: (1) main pyroclastic cone, (2) lava flow fields with abundant rafted cone material, and (3) lava flow fields with little pyroclastic surface material. These three surfaces provided different initial conditions for subsequent geomorphic evolution, as summarized in Figure 12, and they add a level of complexity to the landscape evolution scheme of Wells et al. (1985).

Posteruptive degradation of the main cones (Fig. 12A) begins with development of rills on cone slopes. Initiation of rilling requires low-permeability areas on the cone surface that enable runoff of rainwaters rather than simple infiltration into loose scoria. At cones that are characterized by closing stages of violent Strombolian activity, such as Lathrop Wells volcano (Valentine et al., 2005; Valentine and Harrington, 2006), a significant period of time, perhaps many tens of thousands of years, may be required as eolian sediment and carbonate clog pore spaces in loose surface scoria, finally reducing its permeability sufficiently to stop rain infiltration. At the Pleistocene Crater Flat volcanoes, however, the presence of large bombs and densely welded spatter facies from closing pyroclastic eruptions may have provided impermeable surfaces such that runoff and rilling began relatively quickly. Formation and downcutting of rills transport pyroclastic material downward to a growing apron around the base of the cone. As pedogenic processes clog the upper horizon of the reworked apron, it in turn becomes relatively impermeable to rainwater, such that runoff nucleates and forms rills in the apron, transporting pyroclasts farther away from the cone. This multistage process presumably continues until the cone topography is quite subdued.

Lava fields with abundant mounds of pyroclastic material (Fig. 12B) develop drainage networks by a combination of headward erosion of gullies that initially nucleate between marginal lava lobes, and development of rills on mound slopes that converge to form gullies in low areas between mounds. The resulting networks transport pyroclastic debris to the distal edges of the lava field, where it accumulates as small alluvial fans and aprons. These aggradational features obscure the primary features of the lava margins (e.g., flow lobes, steep flow fronts). This contrasts with a lava field that has few or no pyroclast mounds and little or no fallout lapilli on its surface (Fig. 12C), which undergoes processes of smoothing on the top of the platform and gullying that begins only between flow lobes at its margin with slow headward erosion. Such a lava field may retain its steep flow fronts and other lava structures much longer than a pyroclast mound-rich lava field. This points out the importance of accounting for different initial conditions of surfaces when determining relative ages based on modern morphology. Bradshaw and Smith (1994) inferred that the different morphologies of the two lava fields each at Red Cone and Black Cone volcanoes represented significant gaps in time between emplacement of the lavas (although not specified by Bradshaw and Smith, 1994, such differences would imply time gaps of many tens to hundreds of thousands of years), but we argue that the differences primarily reflect different initial characteristics of the lava fields.

Posteruptive surficial processes also provide an explanation for the morphology of pyroclast mounds, most of which have subdued, rounded shapes and abundant coarse pyroclastic material on their tops. There are probably many different types of rafts (e.g., see Gutmann, 1979; Holm, 1987; Luhr and Simkin, 1993): Figure 13 shows postemplacement evolution of three different types: (1) raft with intact cone bedding (e.g., Holm, 1987), (2) raft of agglutinate deposits that have partly disintegrated during transport on top of a lava, and (3) raft of initially unconsolidated, loose pyroclastic debris blanketed by scoria fallout. These different types of rafts can evolve to mounds with similar appearances that do not on the surface show much of their original character, due to mechanical weathering and accumulation of eolian sediment.

CONCLUSIONS

The Pleistocene volcanoes in Crater Flat were formed by a range of explosive processes including Strombolian and, potentially, violent Strombolian explosive activity. These were

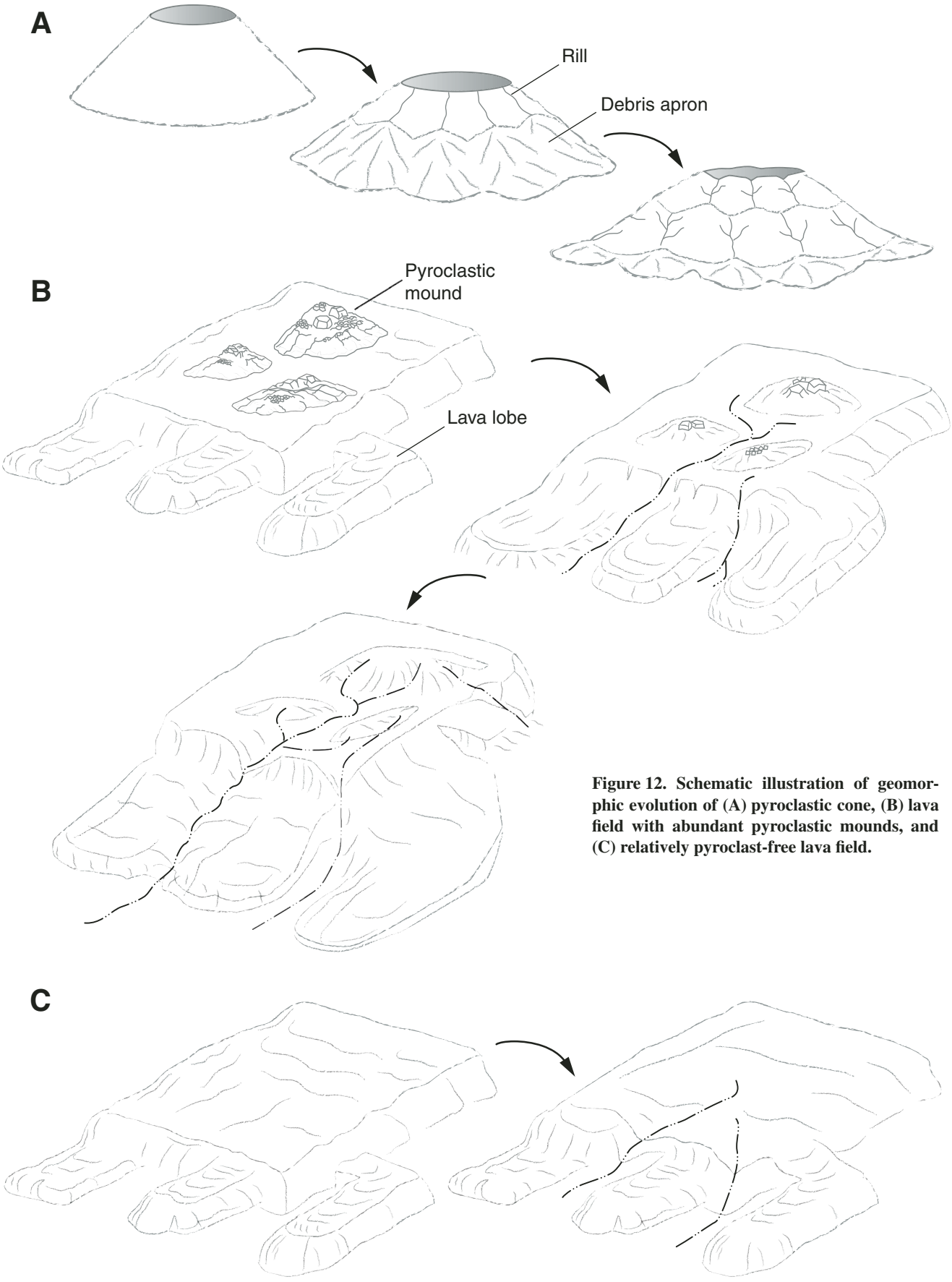

Figure 12. Schematic illustration of geomorphic evolution of (A) pyroclastic cone, (B) lava field with abundant pyroclastic mounds, and (C) relatively pyroclast-free lava field.

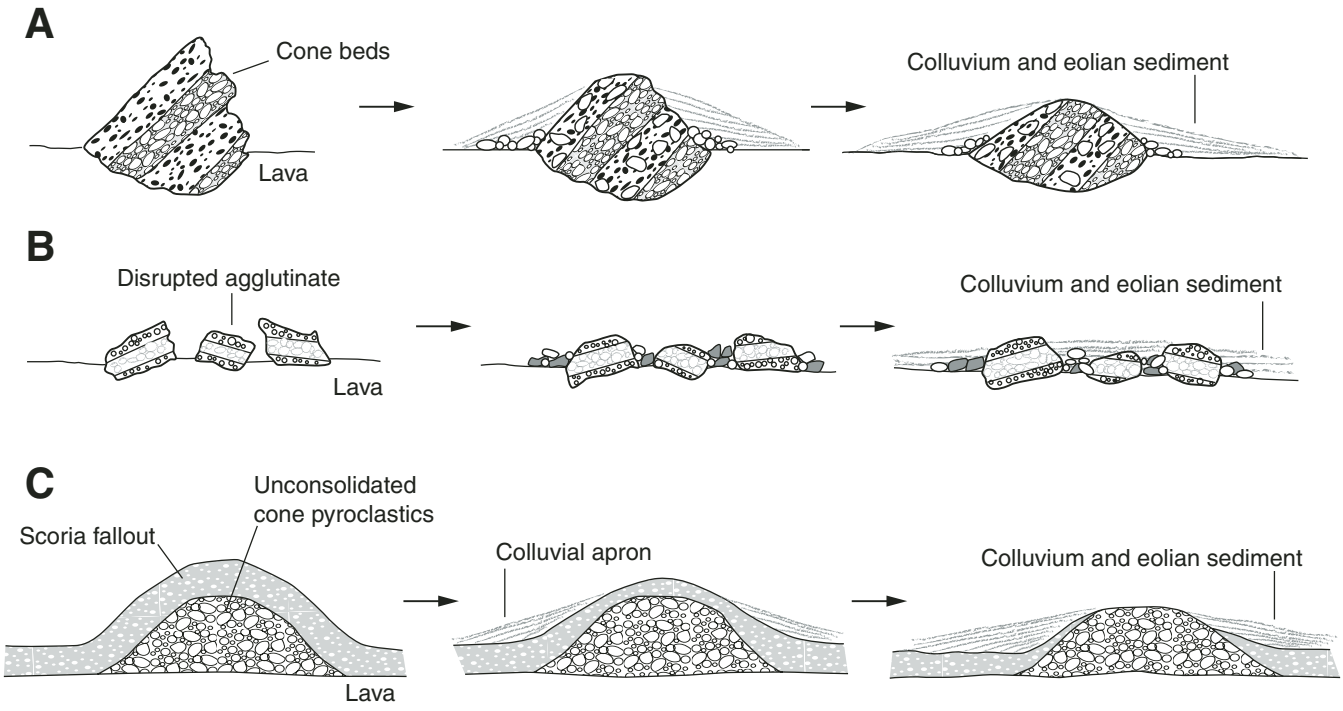

Figure 13. Illustration of postemplacement evolution of pyroclastic mounds that originate as rafted cone material. (A) Raft is emplaced with cone bedding still intact. Gully exposure of tilted beds shown in Figure 7A is an example of this type of mound. (B) Raft of partly welded agglutinate that disintegrated into large blocks during emplacement. Station BC-13 is an example of this type of mound. (C) Raft emplaced as loose, coarse pyroclastic material subsequently covered with fallout lapilli. Note that the top and middle raft types could also be mantled (except on initially steep faces) with fallout lapilli, which would modify their geomorphic evolution somewhat. As time progresses the initially different types of pyroclastic mounds grow increasingly similar in appearance due to surficial processes.

accompanied by development of lava fields that thickened through a combination of flow unit stacking and inflation, expanding laterally in a manner determined by the interplay between effusion rates and paleotopography. Cone growth, cone deconstruction by failure of cone segments and rafting atop lava flows, and cone healing were intimately linked and resulted in complex histories preserved in cone remnant deposits. The volcanoes are monogenetic, and geochemical variations within individual volcanoes (Bradshaw and Smith, 1994; Perry et al., 1998) should be interpreted within that framework (e.g., Strong and Wolff, 2003) rather than invoking long time gaps. Posteruptive geomorphic evolution in this arid to semiarid region was strongly influenced by the characteristics of the original volcanic surfaces, thus complicating any relative age determinations based upon erosional characteristics of different volcanic features. We suggest that volcanic surfaces, such as described in this paper, coupled with well-constrained radiometric age dating provide an avenue for future research into the role of initial surface properties on geomorphic processes in arid settings (e.g., Valentine and Harrington, 2006).

A final note pertains to volcanic risk assessment. If a potential volcanic eruption at the proposed Yucca Mountain repository is similar to the Pleistocene Crater Flat volcanoes and to the Lathrop Wells volcano, the results presented here indicate that the event would consist of one main feeder conduit forming a main cone with shallow lava breakouts (boccas) around the base of that cone, and a duration of ~1–3 yr based upon effusion rates estimated above. This contrasts with previous interpretations (Vaniman and Crowe, 1981; Bradshaw and Smith, 1994) that imply multiple feeder conduits (based upon their inferences that pyroclast mounds each represent separate vents) and long gaps in time between polycyclic eruptions. These conclusions will be incorporated into future risk assessments, which require calculation of the geometry and effects of volcanic eruptions penetrating a repository at depths of ~250–350 m. Volcanic risk assessments for urban areas in basaltic volcanic fields (e.g., Mexico City and Auckland, New Zealand; Valentine, 2003) will require similar characterization of the processes associated with small basaltic volcanoes.

ACKNOWLEDGMENTS

We thank David Vaniman, Nancy Riggs, Michael Ort, Karl Karlstrom, Mike Cline, an anonymous reviewer, and Chuck Harrington for reviewing the manuscript. Figures were prepared by Andrea Kron. This work was supported by the U.S. Department of Energy's Yucca Mountain Project, which is managed by the Bechtel-SAIC Company.

REFERENCES CITED

Bradshaw, T.K., and Smith, E.I., 1994, Polygenetic Quaternary volcanism at Crater Flat, Nevada: Journal of Volcanology and Geothermal Research, v. 63, p. 165–182, doi: 10.1016/0377-0273(94)90072-8.

Cande, S.C., and Kent, D.V., 1995, Revised calibration of the geomagnetic polarity time scale for the Late Cretaceous and Cenozoic: Journal of Geophysical Research, v. 100, p. 6093–6095, doi: 10.1029/94JB03098.

Connor, C.B., Lane-Magsino, S., Stamatakos, J.A., Martin, R.H., LaFemina, P.C., Hill, B.E., and Lieber, S., 1997, Magnetic surveys help reassess volcanic hazards at Yucca Mountain, Nevada: Eos (Transactions, American Geophysical Union), v. 78, p. 73–78.

Crowe, B.M., 1986, Volcanic hazard assessment for disposal of high-level radioactive waste, *in* Active Tectonics: Washington, D.C., National Academy Press, p. 247–260.

Crowe, B., Self, S., Vaniman, D., Amons, R., and Perry, F., 1983, Aspects of potential magmatic disruption of a high-level radioactive waste repository in southern Nevada: The Journal of Geology, v. 91, p. 259–276.

Dartevelle, S., and Valentine, G.A., 2005, Early-time multiphase interactions between basaltic magma and underground openings at the proposed Yucca Mountain radioactive waste repository: Geophysical Research Letters, v. 32, doi: 10.1029/2005GL024172.

Duncan, A.M., Guest, J.E., Stofan, E.R., Anderson, S.W., Pinkerton, H., and Calvari, S., 2004, Development of tumuli in the medial portion of the 1983 a'a flow-field, Mount Etna, Sicily: Journal of Volcanology and Geothermal Research, v. 132, p. 173–187, doi: 10.1016/S0377-0273(03)00344-5.

Fleck, R.J., Turrin, B.D., Sawyer, D.A., Warren, R.G., Champion, D.E., Hudson, M.R., and Minor, S.A., 1996, Age and character of basaltic rocks of the Yucca Mountain region, southern Nevada: Journal of Geophysical Research, v. 101, p. 8205–8227, doi: 10.1029/95JB03123.

Gutmann, J.T., 1979, Structure and eruptive cycle of cinder cones in the Pinacate volcanic field and the controls of Strombolian activity: The Journal of Geology, v. 87, p. 448–454.

Gutmann, J.T., 2002, Strombolian and effusive activity as precursors to phreatomagmatism: Eruptive sequence at maars of the Pinacate volcanic field, Sonora, Mexico: Journal of Volcanology and Geothermal Research, v. 113, p. 345–356, doi: 10.1016/S0377-0273(01)00265-7.

Head, J.W., and Wilson, L., 1989, Basaltic pyroclastic eruptions: Influence of gas-release patterns and volume fluxes on fountain structure, and the formation of cinder cones, spatter cones, rootless flows, lava ponds, and lava flows: Journal of Volcanology and Geothermal Research, v. 37, p. 261–271, doi: 10.1016/0377-0273(89)90083-8.

Heiken, G., 1978, Characteristics of tephra from Cinder Cone, Lassen Volcanic National Park, California: Bulletin Volcanologique, v. 41, p. 1–12.

Heizler, M.T., Perry, F.V., Crowe, B.M., Peters, L., and Appelt, R., 1999, The age of the Lathrop Wells volcanic center: An $^{40}Ar/^{39}Ar$ dating investigation: Journal of Geophysical Research, v. 104, p. 767–804, doi: 10.1029/1998JB900002.

Holm, R.F., 1987, Significance of agglutinate mounds on lava flows associated with monogenetic cones: An example at Sunset Crater, northern Arizona: Geological Society of America Bulletin, v. 99, p. 319–324, doi: 10.1130/0016-7606(1987)99<319:SOAMOL>2.0.CO;2.

Hooper, D.M., and Sheridan, M.F., 1998, Computer-simulation models of scoria cone degradation: Journal of Volcanology and Geothermal Research, v. 83, p. 241–267, doi: 10.1016/S0377-0273(98)00031-6.

Kilburn, C.R.J., and Lopes, R.M., 1991, General patterns of flow field growth: A'a and blocky lavas: Journal of Geophysical Research, v. 96, p. 19,721–19,732.

Luhr, J.F., and Housh, T.B., 2002, Melt volatile contents in basalts from Lathrop Wells and Red Cone, Yucca Mountain Region (SW Nevada): Insights from glass inclusions: Eos (Transactions, American Geophysical Union), v. 83, abs. V22A–1221.

Luhr, J.F., and Simkin, T., eds., 1993: Paricutín, the Volcano Born in a Mexican Cornfield: Phoenix, Geoscience Press, Inc., 427 p.

McFadden, L.D., Wells, S.G., and Jercinovich, M.J., 1987, Influences of eolian and pedogenic processes on the origin and evolution of desert pavements: Geology, v. 15, p. 504–508, doi: 10.1130/0091-7613(1987)15<504:IOEAPP>2.0.CO;2.

McGetchin, T.R., Settle, M., and Chouet, B.A., 1974, Cinder cone growth modeled after Northeast Crater, Mount Etna, Sicily: Journal of Geophysical Research, v. 79, p. 3257–3272.

Nicholis, M.G., and Rutherford, M.J., 2004, Experimental constraints on magma ascent rate for the Crater Flat volcanic zone hawaiite: Geology, v. 32, p. 489–492, doi: 10.1130/G20324.1.

Parfitt, E.A., 2004, A discussion of the mechanisms of explosive basaltic eruptions: Journal of Volcanology and Geothermal Research, v. 134, p. 77–107, doi: 10.1016/j.jvolgeores.2004.01.002.

Perry, F.V., Crowe, B.M., Valentine, G.A., and Bowker, L.M., eds., 1998, Volcanism studies: Final report for the Yucca Mountain Project: Los Alamos, New Mexico, Los Alamos National Laboratory, LA-13478-MS, 554 p.

Perry, F.V., Cogbill, A.H., and Kelley, R.E., 2005, Uncovering buried volcanoes at Yucca Mountain: New data for volcanic hazard assessment: Eos (Transactions, American Geophysical Union), v. 86, p. 485, 488.

Pinkerton, H., and Sparks, R.S.J., 1976, The 1975 sub-terminal lavas, Mount Etna: A case history of the formation of a compound lava field: Journal of Volcanology and Geothermal Research, v. 1, p. 167–182, doi: 10.1016/0377-0273(76)90005-6.

Rossi, M.J., 1997, Morphology of the 1984 open-channel lava flow at Krafla volcano, northern Iceland: Geomorphology, v. 20, p. 95–112, doi: 10.1016/S0169-555X(97)00007-X.

Siebe, C., Rodríguez-Lara, V., Schaaf, P., and Abrams, M., 2004, Radiocarbon ages of Holocene Pelado, Guespalapa, and Chichinautzin scoria cones, south of Mexico City: Implications for archeology and future hazards: Bulletin of Volcanology, v. 66, p. 203–225, doi: 10.1007/s00445-003-0304-z.

Smith, E.I., Feuerbach, D.L., Naumann, T.R., and Faulds, J.E., 1990, Annual report of the Center for Volcanic and Tectonic Studies for the period 10-1-89 to 9-30-90: Carson City, Nevada, The Nuclear Waste Project Office, Report 41.

Stamatakos, J.A., Connor, C.B., and Martin, R.H., 1997, Quaternary basin evolution and basaltic volcanism of Crater Flat, Nevada, from detailed ground magnetic surveys of the Little Cones: The Journal of Geology, v. 105, p. 319–330.

Strong, M., and Wolff, J., 2003, Compositional variations within scoria cones: Geology, v. 31, p. 143–146.

Sumner, J.M., 1998, Formation of clastogenic lava flows during fissure eruption and scoria cone collapse: The 1986 eruption of Izu-Oshima volcano, eastern Japan: Bulletin of Volcanology, v. 60, p. 195–212, doi: 10.1007/s004450050227.

Sumner, J.M., Blake, S., Matela, R.J., and Wolff, J.A., 2005, Spatter: Journal of Volcanology and Geothermal Research, v. 142, p. 49–65.

Valentine, G.A., 2003, Towards integrated natural hazards reduction in urban areas, *in* Heiken, G., Fakundiny, R., and Sutter, J., eds., Geosciences in the Cities: Washington, D.C., American Geophysical Union Special Publication Series 56, p. 63–74.

Valentine, G.A., and Groves, K.R., 1996, Entrainment of country rock during basaltic eruptions of the Lucero volcanic field, New Mexico: The Journal of Geology, v. 104, p. 71–90.

Valentine, G.A., and Harrington, C.D., 2006, Clast size controls and longevity of Pleistocene desert pavements at Lathrop Wells and Red Cone volcanoes, southern Nevada: Geology, v. 34, p. 533–536.

Valentine, G.A., Krier, D., Perry, F.V., and Heiken, G., 2005, Scoria cone construction mechanisms, Lathrop Wells volcano, southern Nevada, USA: Geology, v. 33, p. 629–632, doi: 10.1130/G21459.1.

Vaniman, D., and Crowe, B., 1981, Geology and petrology of the basalts of Crater Flat: Applications to volcanic risk assessment for the Nevada Nuclear Waste Storage Investigations: Los Alamos, New Mexico, Los Alamos National Laboratory, LA-8845-MS, 67 p.

Vaniman, D.T., Crowe, B.M., and Gladney, E.S., 1982, Petrology and geochemistry of hawaiite lavas from Crater Flat, Nevada: Contributions to Mineralogy and Petrology, v. 80, p. 341–357, doi: 10.1007/BF00378007.

Walker, G.P.L., 1973, Lengths of lava flows: Philosophical Transactions of the Royal Society of London, ser. A, v. 274, p. 107–118.

Wells, S.G., Dohrenwend, J.C., McFadden, L.D., Turin, B.D., and Mahrer, K.D., 1985, Late Cenozoic landscape evolution on lava flow surfaces of the Cima volcanic field, Mojave Desert, California: Geological Society of America Bulletin, v. 96, p. 1518–1529, doi: 10.1130/0016-7606(1985)96<1518:LCLEOL>2.0.CO;2.

Wells, S.G., McFadden, L.D., Renault, C.E., and Crowe, B.M., 1990, Geomorphic assessment of late Quaternary volcanism in the Yucca Mountain area, southern Nevada: Implications for the proposed high-level radioactive waste repository: Geology, v. 18, p. 549–553, doi: 10.1130/0091-7613(1990)018<0549:GAOLQV>2.3.CO;2.

Wood, C.A., 1980a, Morphometric evolution of cinder cones: Journal of Volcanology and Geothermal Research, v. 7, p. 387–413, doi: 10.1016/0377-0273(80)90040-2.

Wood, C.A., 1980b, Morphometric analysis of cinder cone degradation: Journal of Volcanology and Geothermal Research, v. 8, p. 137–160, doi: 10.1016/0377-0273(80)90101-8.

Wood, Y.A., Graham, R.C., and Wells, S.G., 2002, Surface mosaic map unit development for a desert pavement surface: Journal of Arid Environments, v. 52, p. 305–317, doi: 10.1006/jare.2002.1006.

Wood, Y.A., Graham, R.C., and Wells, S.G., 2005, Surface control of desert pavement pedologic process and landscape function, Cima volcanic field, Mojave Desert, California: CATENA, v. 59, p. 205–230.

Manuscript Received 20 December 2005
Revised Manuscript Received 8 May 2006
Manuscript Accepted 4 June 2006

Printed in the USA